frontiers | Frontiers in Earth Science

TYPE Original Research
PUBLISHED 10 October 2024
DOI 10.3389/feart.2024.1434785

OPEN ACCESS

EDITED BY
Hongjian Zhu,
Yanshan University, China

REVIEWED BY
Walter D'Alessandro,
National Institute of Geophysics and Volcanology, Section of Palermo, Italy
Gilles Levresse,
National Autonomous University of Mexico, Mexico

*CORRESPONDENCE
D. T. Halford,
d.t.halford@gmail.com

RECEIVED 18 May 2024
ACCEPTED 09 September 2024
PUBLISHED 10 October 2024

CITATION
Halford DT, Karolytė R, Dellenbach JT, Cathey B, Cathey M, Balentine D, Andreason MW and Rice GK (2024) Applications in utilizing soil gas geochemistry along with geological and geophysical data to construct helium exploration statistical models.
Front. Earth Sci. 12:1434785.
doi: 10.3389/feart.2024.1434785

Applications in utilizing soil gas geochemistry along with geological and geophysical data to construct helium exploration statistical models

D. T. Halford[1]*, R. Karolytė[2], J. T. Dellenbach[3], B. Cathey[4], M. Cathey[4], D. Balentine[5], M. W. Andreason[6] and G. K. Rice[5]

[1]Department of Earth Sciences, University of Oxford, Oxford, United Kingdom, [2]Snowfox Discovery, Oxford, United Kingdom, [3]Division of Energy and Mineral Development, Lakewood, CO, United States, [4]Earthfield Technology LLC, Richmond, TX, United States, [5]GeoFrontiers Corporation, Rowlett, TX, United States, [6]Navajo Nation Oil and Gas Company, St. Michaels, AZ, United States

A key challenge in helium (He) exploration is determining the efficacy of surficial soil gas surveys. While soil gas surveys can detect helium, the mechanisms leading to these signals are often poorly understood, hindering reliable interpretation for exploration purposes. Here we present the results of seven new He soil gas surveys (n = 1974) at the Akah Nez Field, Beautiful Mountain Field, Porcupine Dome area, Rattlesnake Field, Tom area, Tohache Wash area, and White Rock area, on the Colorado Plateau, Four Corners area, United States. Utilizing 2D seismic, well logs, and geophysical potential field data, structural maps were constructed of potential He reservoirs at depth and relationships were examined. Given geospatial relationships are being examined using the soil gas survey data, it is important to understand the mechanism that allows subsurface He to migrate upwards into the soil. In several fields interpreted basement faults act as migration conduits from the basement to the surface (i.e., leaky reservoir seals), and in other cases there is evidence for reservoir flank/crest fracturing likely due to differential compaction. Based on the regional geologic history, advective systems are likely responsible for the observed He soil gas signatures. Additionally, based on the Tohache Wash data (most prospective He area) an effective and risk-reducing novel technique is presented that constructs a predictive He exploration model utilizing soil gas geochemistry, high-resolution geophysical data, well data and seismic data using Bayesian ANOVA techniques, which may be translated to areas outside of the Four Corners area, United States.

KEYWORDS

helium exploration, geophysics, geochemistry, statistics, soil gas, structural geology

Highlights

- We find reservoir fracturing is likely due to differential compaction and that He migration conduits can be linked from depth to surface.
- We propose that advection-driven systems (migration via faults/fractures) are likely responsible for the observed He soil gas signatures.
- We present a risk reducing and novel technique to construct a predictive He exploration model utilizing Bayesian ANOVA techniques.

1 Introduction

The utility of soil gas geochemistry as an exploration tool to distinguish geochemical anomalies is a cost-effective and relatively rapid method to search for surficial gas seepages, quantify lateral extent of anomalies, and obtain clues about potential subsurface accumulations (Rice, 2022). Given the extremely cheap overall cost of soil gas sampling, it can be employed on a large scale and cover wide swathes of land. Despite the inability to differentiate isotopes compared to more advanced isotope geochemical analysis (which can be useful in determining information about sourcing, mixing and migration of subsurface fluids, (Ballentine et al., 2002; Macintosh and Ballentine, 2012), the utility of soil gas geochemistry is more focused on geospatially marking the boundaries of gas anomalies (areas with signatures above background) and quantifying the lateral extent of a subsurface reservoir (Andreason et al., 2022).

There are numerous models describing the migration pathways of helium (He) from its predominately basement source rock upwards into overlying sediments (Boreham et al., 2018; Buttitta et al., 2020; Cheng et al., 2021; Karolyte et al., 2022; Halford et al., 2022; Halford, 2023; Cheng et al., 2023), but none focus specifically on the mechanism that can explain mass transport of He from a reservoir to the surface given realistic geologic timelines for a tectonically active area. This is important because understanding the transport mechanism can allow a deeper understanding of the migration and trapping mechanisms of He-systems. Therefore, understanding the migration of He from subsurface reservoirs to the surface can aid in the refinement of pre-existing exploration models and the creation of new approaches to obtain information about reservoirs without costly drilling (Rice, 2022). In this study we test the hypothesis that He soil gas geochemistry surveys can be a cost-effective asset when combined with subsurface geophysical and geological parameters to define/de-risk He-rich regions (i.e., test overall He reservoir potential), which may be translated to other areas beyond the immediate area of the soil gas data.

2 Geologic background

The field area (i.e., Four Corners area) is located on the Colorado Plateau, United States and despite the plateau's relative stability throughout geologic history, it has experienced neotectonism associated with the subduction of the Farallon plate and the subsequent Laramide orogeny (Davis and Bump, 2009). These regional tectonic episodes have produced structural features such as folds, faults, shear zones, and monoclines along with igneous zones in and around the plateau (Craddock et al., 2017; Gonzales and Lake, 2017; Re, 2017). The two major structural features where the sampled fields are located are the Four Corners Platform and the Defiance Uplift (Woodward and James, 1973). The Four Corners Platform, which is a structural high trending northeast that has several anticlines and domes within its boundaries, straddles the Blanding Basin to the northwest and the San Juan Basin to the southeast (Woodward and James, 1973; Woodward et al., 1997). The Defiance Uplift, which is an asymmetrical northern trending uplift marked with numerous folds and some areas of high angle faulting, is bounded by several prominent monoclines to the east and west (Woodward and James, 1973). Having established the regional tectonic background, a more localized description of the field areas of interest is next presented.

The Tohache Wash area, which has He concentrations by volume of up to 6%, is located in north-eastern Arizona on the southwest edge of the Four Corners Platform (Spencer, 1978) (Figure 1). The Rattlesnake Field, which has He up to ~7%, is located in north-western New Mexico on the Four Corners Platform (Baars, 1983). The White Rock area, which is located 1.6 km east of the Arizona-New Mexico state border in San Juan County, New Mexico, has nearby He shows of 7.8% (Brennan et al., 2021). The Beautiful Mountain Field, which has He up to 5.35%–7%, is a large north-south structurally closed anticline located on the eastern flank of the Defiance Uplift in New Mexico (Brown, 1978; Broadhead and Gillard, 2004). The Porcupine Dome area, which is located on the Four Corners Platform, is located 3.2 km south of the Beautiful Mountain Field in San Juan County, New Mexico and its He % is unknown. The Tom area, which is located 8 km south of the Porcupine Dome area in San Juan County, New Mexico on the southernmost portion of the Four Corners Platform, has He shows of up to 7% (average 5%) (Malinowski, 1983). The Akah Nez Field, which is located on the eastern portion of the Defiance Uplift, is located 14.5 km southwest of the Tom area in San Juan County, New Mexico (Dawson 1983). There are no exact He data for Akah Nez field, however there is a He show located ~5 km to the northwest of the area with He up to ~6% (Brennan et al., 2021; Andreason et al., 2022).

He-rich zones in the fields of interest are concentrated primarily in Paleozoic lithologies. The two most prominent reservoirs in this work are the 1) Mississippian Leadville Limestone that is likely sealed by overlying shales of the Molas Formation (Chidsey, 2020) or impermeable carbonate layers within the Leadville (Halford, 2018), and 2) the Permian Organ Rock Formation which is likely sealed by shales within the Organ Rock Formation (Allis et al., 2003). Generalized San Juan structural province stratigraphy (Brister and Price, 2002) is shown in the Supplementary Figure S1. Working from north to south, the geology, reservoir information, and production history of the areas of interest are described in Supplementary Information S1.

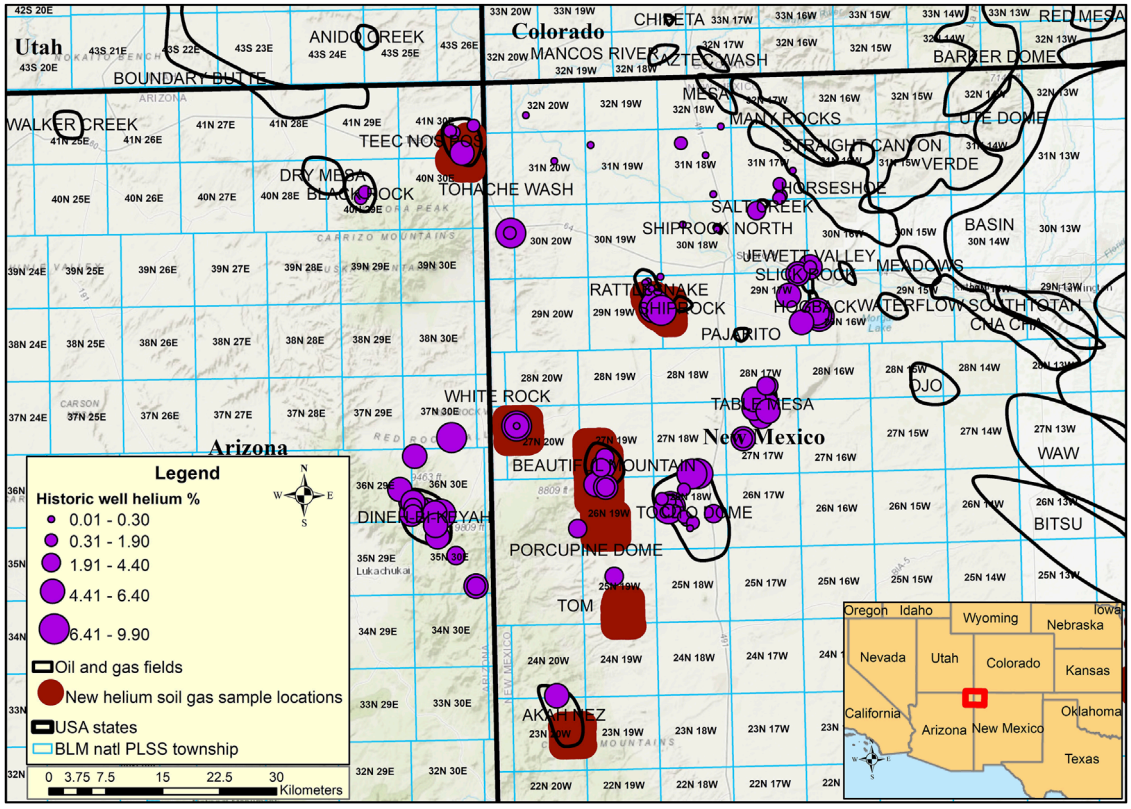

FIGURE 1
Field area showing the seven areas that soil gas surveys were collected in Arizona and New Mexico, United States (Brennan et al., 2021; Halford et al., 2022; Andreason et al., 2022; Halford, 2023).

3 Methods

3.1 Soil data sample collection

Soil gas had been collected from multiple locations to represent several potential He-systems (e.g., known, depleted, unknown) (Andreason et al., 2022). To measure responses over known He accumulations, the Tohache Wash area (6% He) was sampled. To measure responses over partially depleted reservoirs, samples were collected over the Rattlesnake Field (7% He). To measure responses over relatively unknown and sparsely drilled areas (i.e., 1-2 wells per area), the Akah Nez (6% He), Porcupine Dome (He unknown), Tom (5% He), and White Rock 5% He) areas were sampled. Also, gas samples were collected over the Beautiful Mountain Field (5.5%–7% He) because it represents an area with both a depleted reservoir (Leadville) and also a potential undrained discontinuous Organ Rock sandstone reservoir (Andreason et al., 2022).

Using a modified engine powered soil auger probe, He soil gas had been collected at approximately 200 m intervals along transects over seven natural gas fields of interest (Andreason et al., 2022). Once the soil auger probe was at its desired depth (~0.5–1 m), 20 cc of soil gas was withdrawn with a syringe and discarded which effectively flushed the previous samples from the probe as the 20 cubic centimeters (cc) gas volume is 1.5 times the internal sample volume of the probe. Next, another 20 cc of new soil gas was collected with a syringe. This sample was subsequently injected into an evacuated glass sample bottle and stored for no more than 2 weeks before measurements were made. General quality assurance tests included testing for leaks to mitigate air contamination, replacing the septum on the sample collection port, and conducting routine background atmospheric gas measures to monitor background He levels (Andreason et al., 2022).

3.2 Soil gas laboratory analysis

Geochemical analysis solely for He had been completed by GeoFrontiers Corp. with a model 120SSA mass spectrometer based on work completed by the United States Geological Survey (Fridman and Denton, 1976; Reimer, 1976; Andreason et al., 2022). Continuous measurement of ^{4}He was made possible by the fixed mass to charge ratio of the instrument. Using a modified inlet, an aliquot of soil gas was injected. Impurities were separated with a liquid nitrogen cooled trap, and the sample moved to the mass spectrometer where the gas was ionized and components were separated according to their mass/charge ratio. The system was designed to only detect ^{4}He via a specific selection slit which allowed helium ions to pass through to a collector and which produced a current that was proportional to the He concentration interacting with the detector plate. The helium signal was converted to a voltage

and amplified before undergoing integration (i.e., summation of output peaks) to calculate peak areas. Known bracketed He standards were run to establish a reference from which He soil gas concentrations were calculated for each sample (Holland, 1984; Andreason et al., 2022).

3.3 Geophysical mapping methods

Regional lineament density maps had been created by Earthfield Technology LLC by overlaying different lineaments from topographic data, gravity data, magnetic data, interpreted basement faults and interpreted igneous bodies (Andreason et al., 2022). As geomorphology based analyses of surface expressions can often lead to insights about subsurface geology, a Shuttle Radar Topography Mission 30 m digital elevation model was used to generate topographic lineaments. Bouguer gravity lineaments, which were generated using gridded Bouguer gravity data, used subsurface density contrasts of lithologic units to infer information about potential fracturing/faulting. Reduction to the pole (RTP) magnetic lineaments, which were generated using gridded RTP magnetic data, illustrated magnetic contrasts namely by the concentrations of ferromagnetic minerals in the subsurface. Basement faults/lineaments were generated by Earthfield's depth to basement mapping using Werner Deconvolution analysis of gravity and magnetic data (Werner, 1953). Also, utilizing Werner Deconvolution along with filters and derivative maps of magnetic data, the locations and geometries of igneous bodies were derived from magnetic data. Thus, to produce the linear density map, which is a visualization of the number of predicted lineaments, a variety of independent lineaments interpreted from geophysical data were gridded and added via a Boolean gridding process. To produce the intersection density map, areas of pervasive predicted fractures were illustrated by filtering to only illustrate areas where more than three datasets indicated possible fracturing. Directional data were filtered to capture and to enhance structural trends in a particular direction (i.e., N-S, E-W, NW-SE, and SW-NE). More specifically, sharp and distinctive gradients were identified and mapped because they often represent faulting and fracturing that are key in constructing a regional lineament and intersection density map (Andreason et al., 2022).

3.4 Preliminary geological mapping

In order to understand the localized role of structural geology on He accumulations in the area of interest, structure and isopach geological maps had been constructed focusing on a variety of Paleozoic target intervals (Devonian-Cambrian, Mississippian, Pennsylvanian, and Permian) (Andreason et al., 2022). Structural contour maps were created by the Navajo Nation Oil and Gas Co. with manual and automated techniques utilizing existing public well log data from the New Mexico and Arizona state oil/gas commissions and 2-D seismic data to determine the tops of He bearing zones or potential He bearing zones (Andreason et al., 2022). New He soil gas concentration point data were subsequently added to the project (Andreason et al., 2022; Halford, 2023). Building on initial manual He soil gas contours (Andreason et al., 2022), new contours were generated via raster interpolation (utilizing spline and spline with barriers methods) from He concentrations after subtracting average He air values from multiple locations all over the field areas. Additionally, other geologic structures (i.e., basement faults, surface faults, basement highs, igneous bodies, and nodes of fracture intersection), which were interpreted from high-resolution geophysical work completed in the area by Earthfield Technology LLC (Andreason et al., 2022; Halford et al., 2024), were digitized and overlain as shapefiles on the structural maps in ArcGIS. Published He percentages from geochemical well datasets from Brennan et al. (2021), Halford et al. (2022) and Halford (2023) were incorporated into the maps. Zones of known production (i.e., proven areas) and known gas-water contact zones from the Navajo Nation Oil and Gas Co. were also added as shapefiles to the geological maps (Andreason et al., 2022).

3.5 Statistical modeling for Tohache Wash

Following on previous work (Halford et al., 2024), which argued for the significance of regional structural features impacting He-system migration and accumulation, a statistical approach was utilized that examined the impact of locally controlled structural features in relation to measured He values from surficial soil gas surveys. More specifically, the soil gas survey data were used to observe the effect of several structural features with more precision (higher resolution) than previously possible (Halford et al., 2022; Halford et al., 2024), which only had access to a regional He % well dataset (Brennan et al., 2021; Halford et al., 2022). Bayesian Analysis of Variance (ANOVA) models were utilized in JASP (JASP Team, 2023) to assess the effects of which geologic features (i.e., categorical-nominal independent variables) were the most significant in explaining the He soil gas data (i.e., dependent continuous variable) at Tohache Wash (most He prospective area). Subsequently, the approach was tested on the surrounding areas.

Similar to traditional ANOVA models from the frequentist framework, the Bayesian ANOVA model allows differences between multiple group means to be analyzed. A key difference is that Bayesian ANOVA allows for the predictive performance of multiple competing models by looking at the model's relative adequacy and the inclusion probabilities of each component (Rouder et al., 2016; Wagenmakers, et al., 2018). More specifically, the Bayesian approach incorporates prior distributions to allow predictions to be made before looking at the data. For this work, the beta binomial ($\alpha = \beta = 1$) prior was applied to the models, which allows uniform distribution over the size of the model given the default hyperparameters (i.e., equal probability) (Clyde, 2008), and a Cauchy prior ($r = 0.5$) was applied to the regression coefficients (Liang et al., 2008; Bayarri et al., 2012; Wagenmakers, et al., 2018). For reproducible results, a seed of 1 was set. Assumptions of homoscedasticity, independence, and normality were considered and generally found to have been met (van den Bergh et al., 2020). An assumption was made that the soil gas He signatures are not being influenced by lateral transport and are experiencing near vertical He migration.

Each of the soil gas points recorded Boolean dummy indicator variables of either 1 or 0, to mark the presence/absence of a feature.

10.3389/feart.2024.1434785

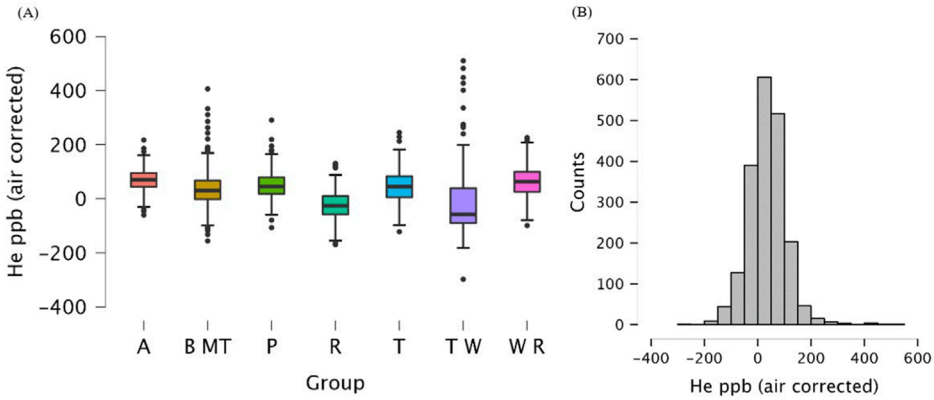

FIGURE 2
(A) Ranges of He in parts by billion (ppb) by volume that have been air corrected (Andreason et al., 2022; Halford, 2023). Sample size and standard deviations are: A, Akah Nez (n = 202, σ = 43.2); BMT, Beautiful Mountain (n = 644, σ = 59.7); P, Porcupine Dome (n = 262, σ = 54.2); R, Rattlesnake (n = 290, σ = 57.5); T, Tom (n = 221, σ = 59.8); T W, Tohache Wash (n = 88, σ = 162.9); and WR, White Rock (n = 267, σ = 56.6). The upper and lower whiskers demarcate the range of data (excluding black point outliers). The upper box represents the 75th percentile, the lower box represents the 25th percentile, and the thick black horizontal line represents the median. **(B)** Normal distribution of data is shown.

TABLE 1 Analysis of effects for coefficients for the Bayesian ANOVA models with He data (n = 88) for the Tohache Wash area.

Effects	P (inclusion)	P (exclusion)	P (inclusion|data)	P (exclusion|data)	$BF_{inclusion}$
Intrusion	0.500	0.500	0.998	0.002	414.711
Reservoir flank	0.500	0.500	0.982	0.018	54.230
Reservoir high	0.500	0.500	0.753	0.247	3.054
Previous He well	0.500	0.500	0.746	0.254	2.935
Basement fault	0.500	0.500	0.656	0.344	1.911
Fracture node	0.500	0.500	0.640	0.360	1.779

For igneous intrusions and fracture nodes, the polygon footprints were used to determine the inclusion/exclusion of the feature. For basement faults, a minimal 200 m buffer was constructed around the feature to determine inclusion/exclusion. For zones demarcating a structural high or flank of a high, approximations were made to correspond to the highest complete structural contour representing the structural high; whereas the flanks were represented by the area from the base of the structural high to the upper most contour (generally up to 1 km). For previous wells, a 200 m buffer was constructed to determine inclusion/exclusion based on the approximate distance of the highest He soil gas contour to the previously drilled He well and to reflect the initial He soil gas sampling 200 m grid.

3.6 Predictive mapping for Tohache Wash

To initiate the predictive model construction, a new fishnet grid was created of equally spaced points every 200 m to reflect the initial spacing of the soil gas survey. Concerning each of the shapefiles and polygons representing the structures of interest, a new field was added to each attribute table in ArcGIS with the respective Bayes factor (BF) inclusion coefficient. For the variables that were recorded as polygons (i.e., intrusions, fracture intersection nodes), a spatial join tool was used to assign values from the fishnet grid to polygons only in overlapping areas. For basement faults, the buffer was increased to 200 m around the feature followed by a spatial join to the new fishnet grid, because the average fracture zone around basement faults is ~200 m. Concerning the reservoir highs, manual areas were still determined based on the highest level of structural contour mapped at a 15 m contour interval. Regarding reservoir flanks, areas were similarly determined based on the structural geology of the Leadville Limestone to distances ~1 km from the crest of the reservoir high. Additionally, areas around previous wells with recorded He shows were drawn with a 200 m radius in each direction surrounding previous wells as the exact drainage area for each well is unknown.

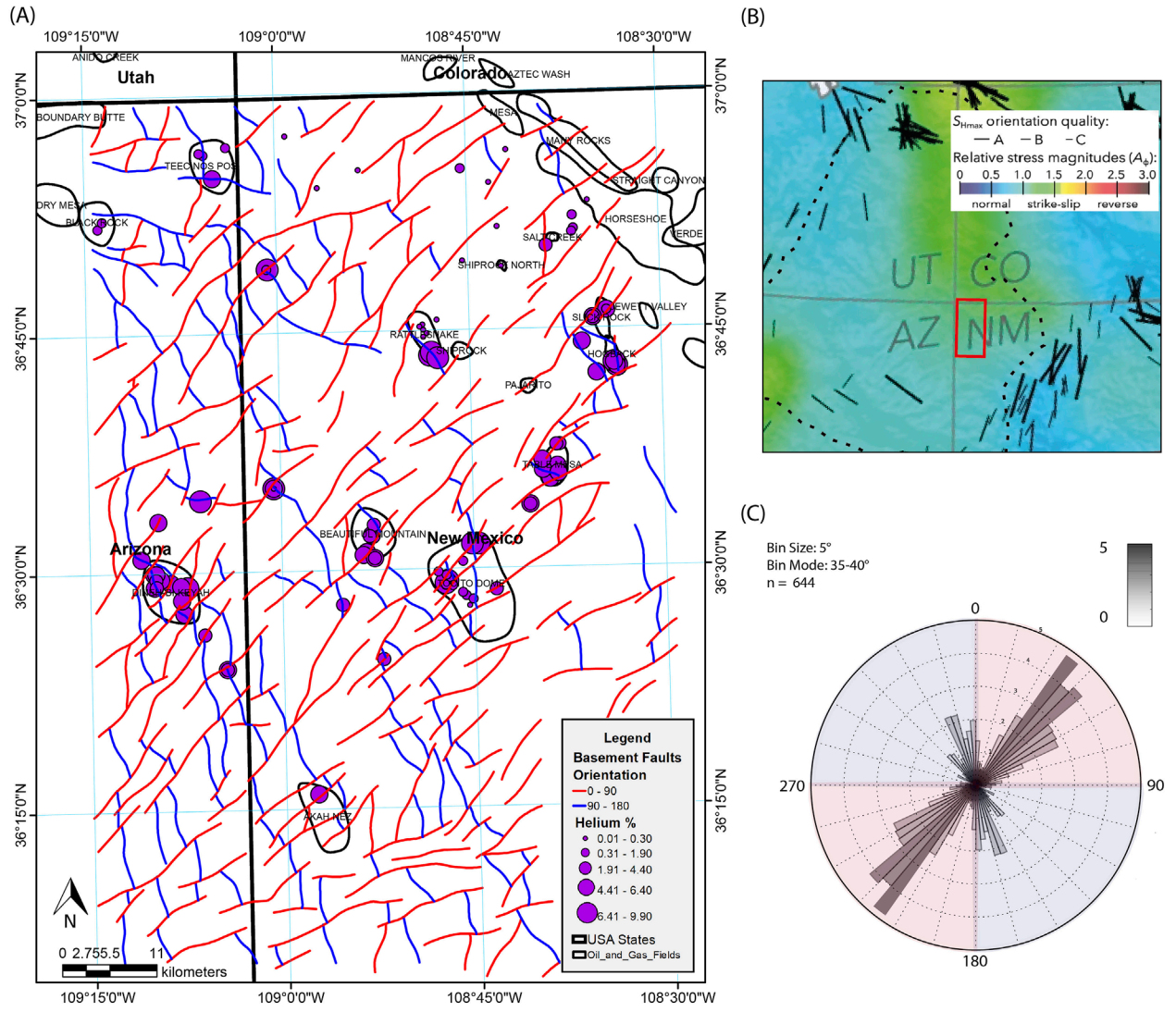

FIGURE 3
(A) Showing an orientation analysis conducted in NetworkGT (Nyberg et al., 2018) with red illustrating basement faults from 0°–90° and blue indicating faults from 90°–180° (mod. From Andreason et al. (2022)) along with overlain He well values (Brennan et al., 2021; Halford et al., 2024); **(B)** Outline of the Colorado Plateau with a dashed black line and red box showing the field area on a state of stress map illustrating maximum horizontal stress (S_{Hmax}) orientations along with relative stress magnitudes (style of faulting) indicated by color (Lunderstern and Zoback, 2020); **(C)** Length weighted fault orientation diagram exhibiting the dominant and longer fault orientation is to the NE and SW.

Next, the computed BF inclusion coefficients were utilized to act as weighting factors for the predictive model and each factor was added based on if a structure or feature was physically present at a specific point. After normalizing the data, the inverse distance weighted (IDW) interpolation method was used to create a contour map of normalized inclusion factor values, which represented a He occurrence prediction map. Therefore, by using Bayesian inclusion coefficients, a prediction model was computed, which was constructed with He data (Brennan et al., 2021; Halford, 2023; Halford et al., 2022) and geologic structural data (Andreason et al., 2022; Halford et al., 2024). The model inputted the predicted variables and translated them into a visual representation of areas where there are ranges of likelihoods of subsurface He gas occurrences.

4 Results

4.1 Soil gas data for all fields

Here we report the He content of (n = 1974) soil gas samples from seven different fields which were chosen to represent case studies of prospective areas and depleted areas for He (Figure 2) (Halford, 2023; Andreason et al., 2022). Data approximately follow the normal distribution for all fields. In order to establish a robust He background value, air samples (n = 30) had been taken which provide a range of 5,240–5,400 ppb, with an average of 5,330 ppb. He measurements were corrected for atmospheric contribution using the established baseline air value of 5,330 ppb. Most areas had He surface signals in the 40–70 s ppb above air range, with the one

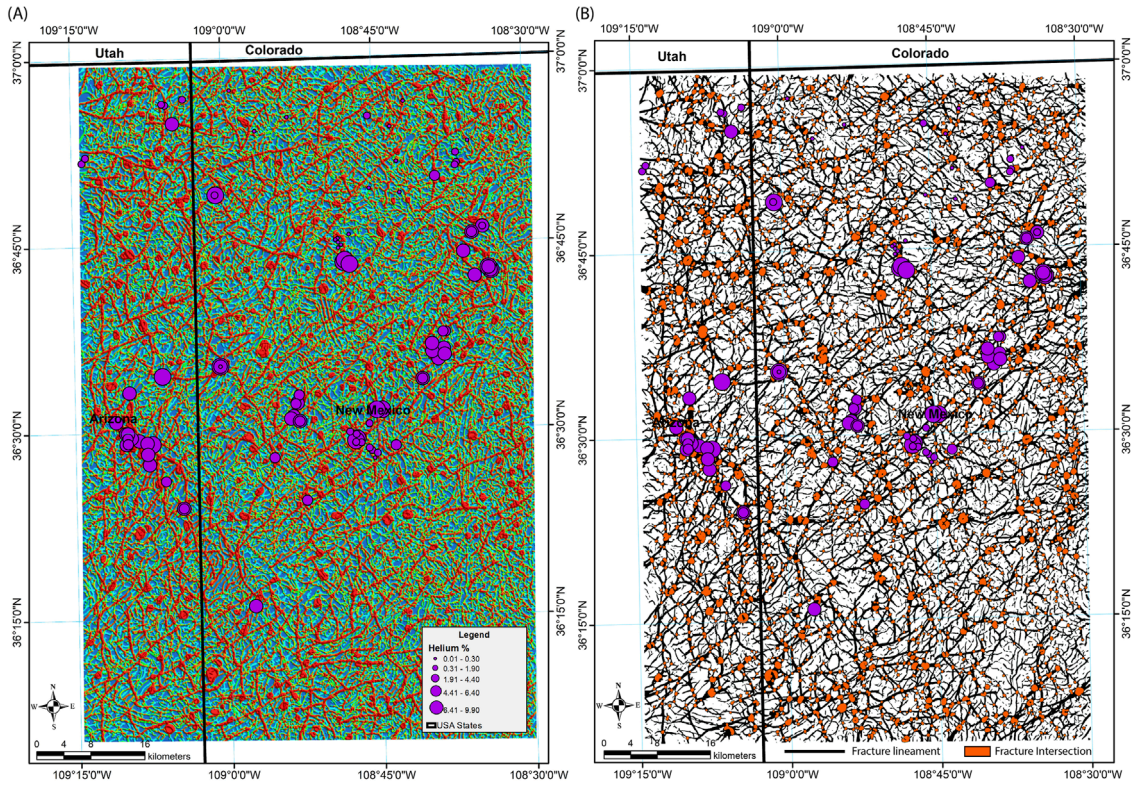

FIGURE 4
(A) Preliminary lineament density map before windowing and directionally filtering lineaments (mod. from Andreason et al. (2022) and **(B)** Interpreted fracture network map and intersections (orange polygons) with He well data (purple circles, Brennan et al., 2021; Halford et al., 2022) showing a complex network of predicted fracturing, courtesy of Earthfield Technology (mod. from Andreason et al. (2022).

exception of the Tohache Wash area with an average He surface signal of 227 ppb above air (Andreason et al., 2022).

4.2 Bayesian statistical models for Tohache Wash

Utilizing the Tohache Wash He data (n = 88), the effects of independent variables (i.e., structural features and historical data – intrusions, basement faults, fracture nodes, reservoir highs, reservoir flanks, and previous He wells) on the dependent variable (i.e., He soil gas values) were examined. The null hypothesis (H_0) is that there is no relationship between the dependent and independent variables. Conversely, the alternative hypothesis (H_1) is that there is a relationship between the dependent He values and independent variables. Bayesian ANOVA models were utilized to simultaneously examine the effects of multiple predictors. The two main outputs from the JASP Bayesian ANOVA module (JASP Team, 2023) are the model comparison charts (Supplementary Tables S1, S2) and the analysis of effects table (Table 1).

We are primarily interested in the Bayes Factors (BF_{10}) (Supplementary Tables S1, S2) and Bayes Factors inclusion coefficients. Regarding the ordering, the Bayes factors (BF_{10}) for each model are shown in Supplementary Table S1 compared to the best model and in Supplementary Table S2 compared to the null model. The BF_{10} measures evidence for the alternative model compared to the null model. Bayes Factors (BF_{10}) of >30 indicate strong evidence in support for the alternative hypothesis (H_1), BF>3 indicate moderate evidence in support of H_1, and BF values of 1–3 indicate weak evidence in support of H_1 (van Doorn et al., 2021). Given the majority of models generated a (BF_{10}) of >30 (i.e., strong evidence for H_1), the observed data are >30 times more likely under the majority of alternative models compared to the null model (Supplementary Table S2).

Examining the analysis of effects table (Table 1), the prior inclusion and exclusion probabilities for all variables are set at 50%. The P (inclusion and exclusion | data) columns show the summed posterior probability for the component of interest averaged over all models. The intrusion and reservoir flank have the highest probabilities of inclusion of 99% and 98%, respectively, after analyzing the data. The BF inclusion factor illustrates the relative change from prior inclusions odds to posterior inclusion odds averaged by all models that include the predictor of interest (van Doorn et al., 2021; JASP Team, 2023). BF inclusion values >1 indicate that the addition of a predictor improves the model (Taouki et al., 2022). BF inclusion factors for the intrusion and reservoir flank predictors are 414.71 and 54.23, respectively, indicating the inclusion of the effects are strongly favored. For example, the observed data are 414.71 times more likely in a model with the intrusion predictor.

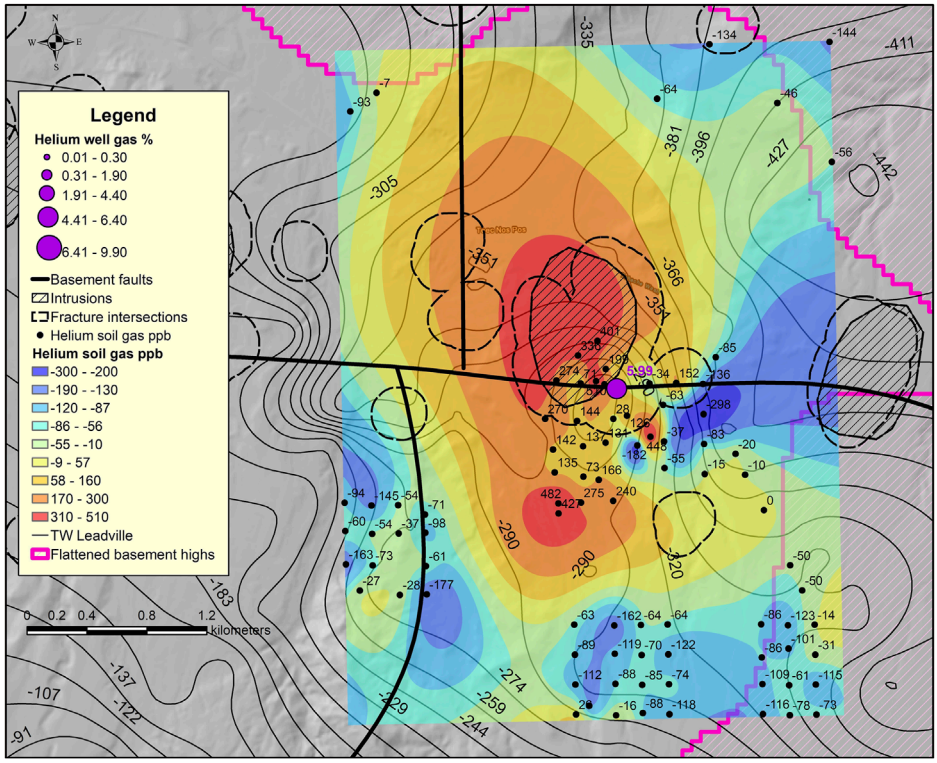

FIGURE 5
Tohache Wash area map showing the He soil gas colored contours (via raster interpolation and manual techniques) of air corrected He soil gas values along with structural elements, He data (Brennan et al., 2021; Halford, 2023) and structural contours (C.I. of 15 m) on top of the Leadville Limestone (mod. from Andreason et al. (2022). There is strong correspondence between He soil gas anomalies and the reservoir structural flank and crest, which could indicate apical (directly above) and halo (spill points) He microseepage.

5 Discussion

5.1 Regional fault and fracture patterns

Previous work (Halford, 2018; Halford et al., 2022; Andreason et al., 2022; Halford et al., 2024) on the Colorado Plateau, illustrates the importance of tectonics (i.e., basement faults and igneous intrusions) in controlling He accumulations by providing and accentuating fault networks (Koide and Bhattacharji, 1975), which can serve as migration conduits for He transport via advective fluid flow. Through examination of various transport mechanisms, the role of faults and fracture networks has been increasingly apparent as a limiting factor for the field area in terms of migration conduits (Halford et al., 2024). To further explore the nature of regional fault significance, regional stress field orientations and fracture network connectivity are examined.

5.1.1 Regional stress field orientation

Using NetworkGT, an in-depth regional fault analysis is completed to examine two-dimensional basement fault networks (n = 644) looking at both geometry and topology attributes (Nyberg et al., 2018). Two fault sets and their respective orientations are presented (Figure 3A). The orientations of basement faults are calculated from each individual fault segments (Nyberg et al., 2018). The dominant orientation, which is from the NE to SW, broadly aligns with the regional stress fields around the Colorado Plateau (Lunderstern and Zoback, 2020) (Figure 3B). Additionally, a maximum horizontal stress orientation of 35° was recorded from a wellbore image log near the Hogback NW of Farmington (Lorenz and Cooper, 2003). The dominant orientation hosts longer faults, which is illustrated by the rose diagram normalized to length (Figure 3C).

To understand the spatial component of historical He wells and fault orientation, a 1 km buffer is created around each of the fault legs (Halford et al., 2024). Over 85% of all economic He data lie within these buffers, and the remaining were manually assigned to the nearest basement fault. When looking at the distribution of He % and fault orientation, two main groups are observed corresponding to the dominant fault set (45°) and secondary set (150°) fracture orientations. The dominant fault orientation hosts ~60% of all the economic He points, while the secondary fault orientation hosts the remaining 40%. The orientation as well as fault length does not correlate with high-He, however both have similar ranges of He data from 0.3 to ~8% He. One noticeable difference between the two data groupings is the dominant fault orientation has a continuous range from 0.3% to 8% He, while the secondary fault orientation group has a data hole (i.e., lack of data) from ~1.5–4 He %. This discrepancy might be due to disparities/biases within the actual data itself or patterns of chemical alteration, or it could be indicating increased dilation of faults as a function of tectonic stress and lithostatic pressures as well as fluid pressures (Lundstern and Zoback, 2020). Theoretically, active He fluxes from basement via open fractures

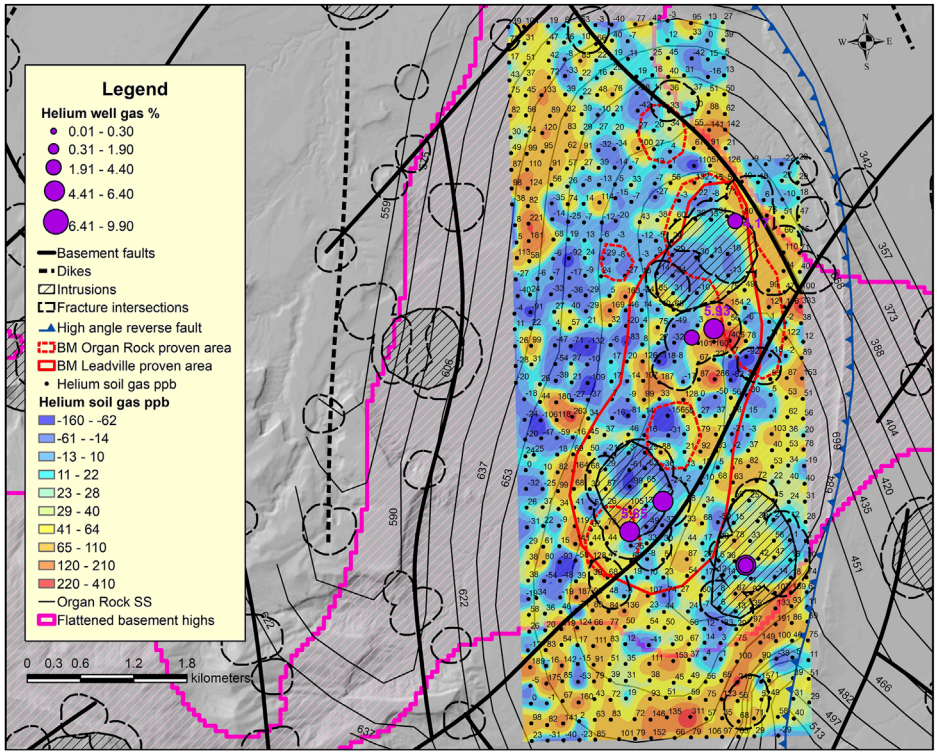

FIGURE 6
Beautiful Mountain Field map showing the He soil gas colored contours (via raster interpolation and manual techniques) of air corrected He soil gas values along with structural elements, He data (Brennan et al., 2021; Halford, 2023), and structural contours (C.I. of 15 m) on top of the Permian Organ Rock sandstone (mod. from Andreason et al. (2022). There is a correspondence between the He soil gas anomalies and a basement fault in the NE portion of the field, which could indicate a pathway-driven microseepage event. The depleted/proven areas of the field are shown related to the Organ Rock and Leadville proven areas, respectively. On the southern portion of the field, He soil gas anomalies occur over potentially undrained portions on the structural flanks of the reservoir, which could indicate halo (spill points) He microseepage or non-produced pockets of gas.

and faults could be inferred in zones where the current regional stress fields align with the interpreted basement fault orientation. This could result in broader and fuller ranges of continuous He anomalies.

5.1.2 High density fracture network

In addition to the basement faults, there is a pervasive fracture network throughout the field area which could be helping or hindering He accumulation potential. Fracture identification (i.e., areas of most pervasive fracturing) was made possible by a complex lineament analysis by combining and integrating lineaments from digital elevation models (topographic lineaments), well data and seismic data (formation lineaments), potential field data (magnetic and gravity lineaments), and basement faults/fractures (magnetic and gravity lineaments), courtesy of Earthfield Technology, LLC (Andreason et al., 2022). Ultimately a lineament and intersection density map, which ties surficial and subsurface lineament expression, was created by combining all the previously described lineaments and shows the number of lineaments predicted in an area (Figure 4A). The final product was produced by combining directionally filtered lineament data and by illustrating the junction of multiple fracture networks to highlight areas of potentially increased natural porosity as a function of interpreted lineament intersection (Figure 4B).

By closely analyzing the distribution of He and the fracture network map, a first order observation is that 94% of economic He (>0.3%) (Brennan et al., 2021; Halford et al., 2022) wells lie on the intersection fracture node (Figure 4B). Of the remaining 6%, half lie on or nearly on a fracture lineament. Fracture intersection nodes are likely zones of increased porosity and permeability, which is why He is observed at these localities. Interestingly, fracture node size does not correlation with higher amounts of He. When analyzing these occurrences to be the result of a chance relationship, a synthetic random point grid is created and compared to the observed economic He data, which shows they are significantly different distributions with only ~7% of random points falling on a fracture intersection node.

Given there are many localities that have fracture intersection nodes but no He anomaly, this supports the statement that fracture nodes are likely important in the He-system facilitating advection based transport, but are not the most important geologic feature in the transportation and accumulation of He in the subsurface. Another observation is the intricate nature of the predicated fracture network and fault intersection map. The Colorado Plateau, which has experienced relatively little to moderate deformation compared to more active geologic regimes (i.e., Yellowstone), is likely extremely fractured in the subsurface.

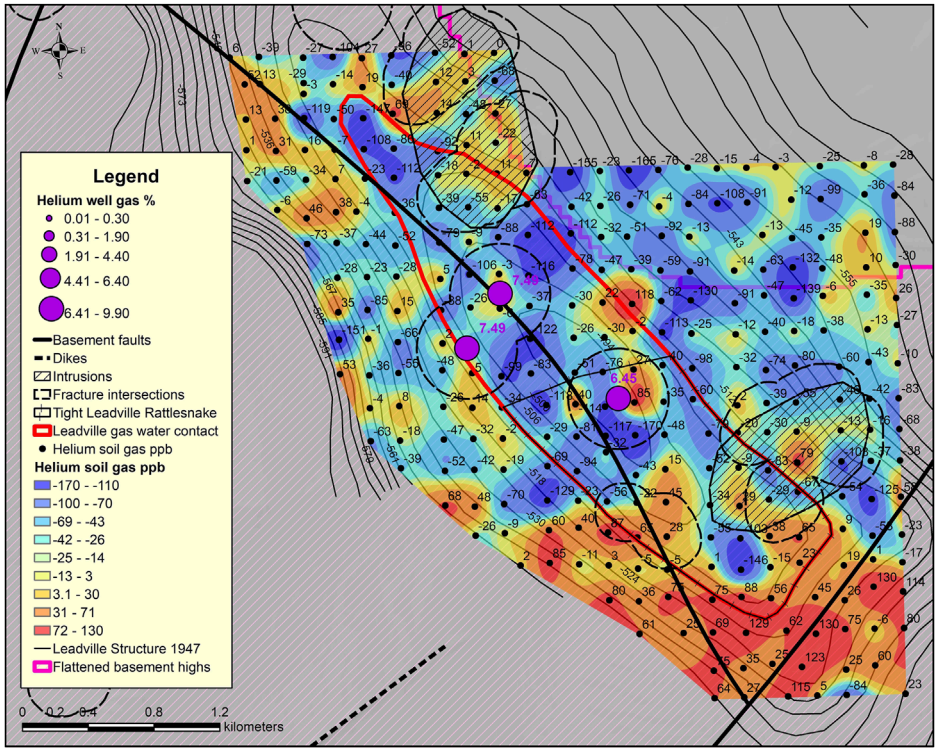

FIGURE 7
The Rattlesnake Field map showing the He soil gas colored contours (via raster interpolation and manual techniques) of air corrected He soil gas values along with structural elements, He data (Brennan et al., 2021; Halford, 2023), and structural contours (C.I. of 15 m) on top of the Mississippian Leadville Limestone (mod. from Andreason et al. (2022). There is a correspondence between the He soil gas anomalies and basement faults on the SE portion of the field, which could indicate pathway-driven advective He microseepage. The overall depleted nature of the field is shown along with the theorized Leadville gas-water contact and tight Leadville areas.

Thus, by using high resolution geophysical data to examine basement fault patterns and potential fracture network intersections, it is observed that 1) basement faults aligned with the regional stress fields are longer and have a more complete range of He anomalies (Figure 3) and 2) there is a strong correlation with fracture network intersections (94%) and economic He wells (>0.3 He %) (Figure 4B). Therefore, understanding mechanisms (e.g., faults and fracture patterns) that can influence He migration/accumulations is critical in understanding the He-system.

5.2 Localized geologic reservoir controls

Transitioning from historic He data from previously published works (Brennan et al., 2021; Halford et al., 2022) showing regional trends and relationships between He and faults/fracture networks, the focus shifts to newly reported soil gas data measured at a localized field scale (Andreason et al., 2022; Halford, 2023). Soil gas data measuring He concentrations were mapped to produce contour maps through interpolation and manual techniques over the fields of interest to identify high He zones. Upon conducting preliminary assessments and reservoir structural mapping, a first order observation is that anomalous He zones are aligned with certain structural features or combinations of structural features (e.g., faults, fracture nodes, intrusions, dikes, basement highs). Reservoir structural maps were created to aid in the examination of the role of subsurface reservoir architecture and positions (i.e., reservoir highs or flanks) and the effect on measured He soil gas values.

As the role of regional faults and fracture networks becomes more apparent, the localized structural controls/mechanisms that influence these migration conduits have yet to be investigated. To further explore the nature of structural geology's significance, the roles that differential compaction and fault leakage processes could have on He surface gas signatures (i.e., explaining the geospatial He dispersion patterns and trends) are examined.

5.2.1 Differential compaction

Differential compaction, which is the process of uneven settling of sediments due to porosity loss, is critical in understanding reservoir architecture and connectivity (Gay et al., 2006a; Gay et al., 2006b; Rusciadelli and Di Simone, 2007; Corcoran, 2008; Ireland et al., 2011; Meng and Hodgetts, 2020). Differential compaction can occur either by dewatering episodes or by vertical loading (i.e., sedimentation). The concept of differential compact by sedimentation is relatively simple, in that after deposition of sediments as more and more overburden is added, the sediments will compact over the underlying rocks and form associated faults and fractures (Williams, 1987; Bjorlykke and Hoeg, 1997; Buczkowski and Cooke, 2004; Xu et al., 2015). More specifically,

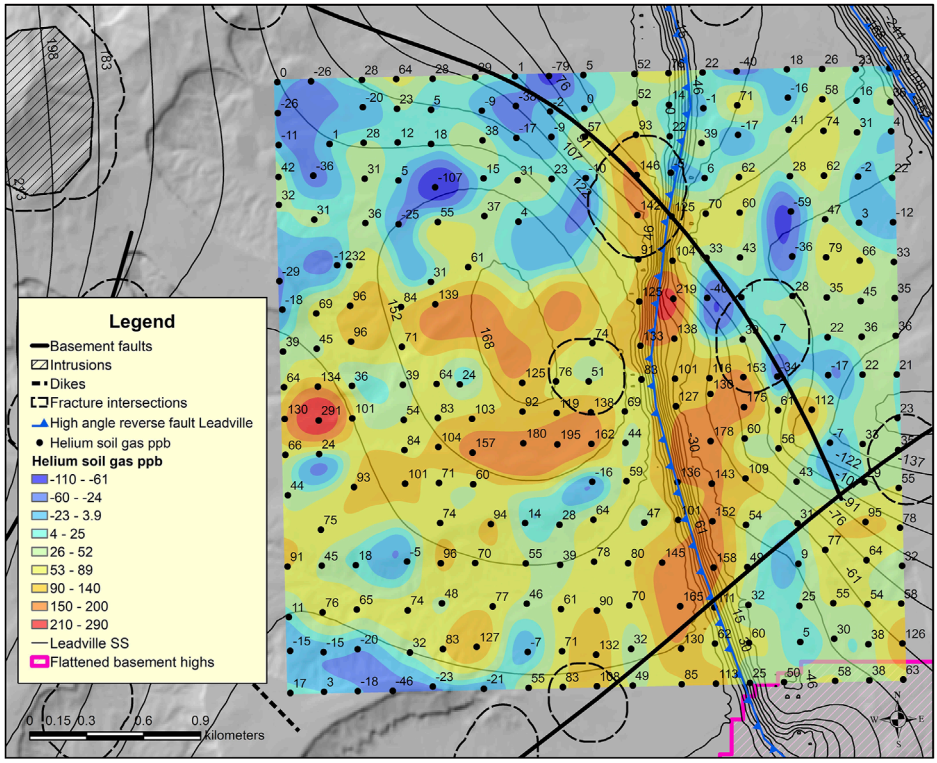

FIGURE 8
The Porcupine Dome area map showing the He soil gas colored contours (via raster interpolation and manual techniques) of air corrected He soil gas values (Halford, 2023) along with structural elements and structural contours (C.I. of 15 m) on top of the Mississippian Leadville Limestone (mod. from Andreason et al. (2022). There is a correspondence between the He soil gas anomalies and a high angle reverse fault on the eastern portion of the field, which could indicate pathway-driven advective He microseepage. Slightly elevated He anomalies around the crest and flank of the structure could also indicate a halo (spill point) He microseepage or fracturing along flanks of the structure.

if there are portions of the underlying geology that protrude and create a circular feature, the weight of the sediments will create an isometric stress field around the protrusions flanks and ultimately lead to differential compaction radial fracturing (Mehl, 1920; Blackwelder, 1920; Moore, 1920; Merriam, 1999; Xu et al., 2015).

We are proposing this mechanism as a contributing reason He anomalies are observed on structural crests and around the flanks of highs. By examining the structure maps of the potential He reservoirs at Tohache Wash (Figure 5), Beautiful Mountain (Figure 6), White Rock (Supplementary Figure S2), Akah Nez (Supplementary Figure S3) and Tom (Supplementary Figure S4), a first-order observation is that there are He soil gas anomalies overlying the flanks of reservoir highs along with several instances of strong crest signatures (Figures 5, 6). In an ideal system, vertical migration theory indicates that natural gas will migrate updip into the crest of a structural high (Rice, 2022). Oftentimes in reality, the natural gas accumulations can be offset from structural crest highs by various features (i.e., gas-water contacts, tight lithologies, tectonic events, fractures/faults, etc.). If the assumption is made that the overlying fracture networks linking up the reservoir to the crust are vertical with minor amounts of lateral offset, it can be argued that this flank signature is derived from differential compaction of sediments. Moreover, the resulting fault or induced fracture pathways (from differential compaction) are either due to a basement high, a rising igneous body, or other underlying geologic features.

5.2.2 Fault leakage

It is well documented that surface hydrocarbon anomalies that are associated with faults often signify a connection to subsurface hydrocarbon reservoirs (Debnam, 1969; Ball and Snowdown, 1973; Dyck, 1976). Translating the principle of microseepage from hydrocarbons to He is a relatively straightforward step (Roberts and Roen, 1985). Whether this association is indicative of a larger accumulation or the tell-tale sign of a transient system with little gas potential is an ongoing debate in the literature (Barry et al., 2013; Mtili et al., 2021; Danabalan et al., 2022). As an aside, to understand how harmful or beneficial a surficial fault seep is, the surface flux of He should be monitored over an extended period of time and not sampled at a singular point for the best odds of success.

By examining the soil gas He signatures, a first-order observation is that the surficial He anomalies generally follow the outline of underlying basement lineaments/faults in the Rattlesnake Field (Figure 7) and to a lesser extent in the Tom area (Supplementary Figure S4). Higher He soil signatures are also observed where a thrust fault cross cuts the Leadville Limestone in the Porcupine Dome area (Figure 8). The presence of He anomalies at the surface indicate that these faults are relatively open and are

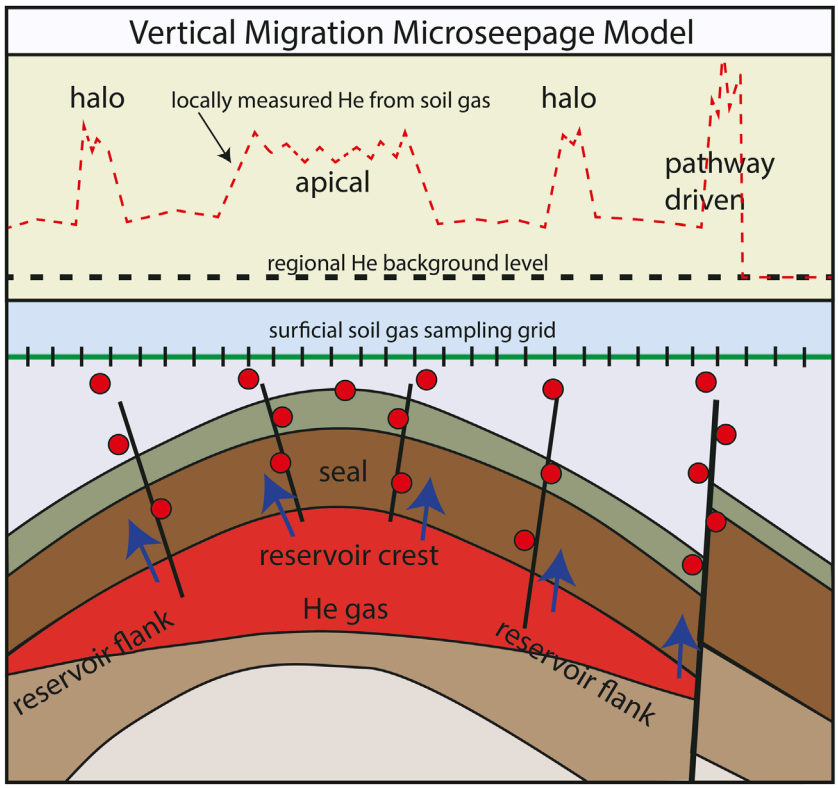

FIGURE 9
The top part of the schematic shows the locally measured He soil gas signatures (red dashed line) relative to a regional background He level (black dashed line) along with the main groupings of observable surface expressions of He gas: 1) pathway-driven, 2) halo, 3) and apical. The bottom of the figure indicates a geologic cross section showing the faults/fractures that are likely responsible for the transport of He gas (red circles), which ultimately influence the observed surficial He soil gas signatures. Advection is the likely transport mechanism for vertical migration related to faults and fractures in and around the reservoir crest/flanks. The size of each anomaly relates to relative flux speed. The pathway-driven seepage example indicates a scenario of an active fault zone from depth to surface where advection dominates transport (modified from Abrams, 2020b; Rice, 2022).

acting as migration conduits (i.e., potential leaky seal). This is a pathway-driven mechanism where the seepage acts to focus He from the reservoir resulting in higher concentrations than surrounding areas. Therefore, He surface gas anomalies that closely resemble lineaments in conjunction with weak and disperse He surface signatures are likely experiencing some degree of rapid advective loss of subsurface He accumulations through faults that are cross-cutting reservoirs. However, it should be noted that if gas loss doesn't outpace the gas sourcing, He accumulations won't be significantly diminished.

5.3 Vertical helium migration from reservoir to surface

As general observations have been discussed of broad mechanisms influencing the geospatial distribution of He concentrations from soil gas data in relation to structural features, next the more detailed processes involved in the mass transport of subsurface He to the surface are discussed.

Vertical migration is an umbrella term describing the mass transport processes that facilitate the movement of gas from subsurface reservoirs to the surface (Rice, 2022). The idea of methodically tracing back surficial seeps to underground reservoirs has been a core approach from the beginnings of hydrocarbon exploration to the present day. More recently, this approach been adapted to He exploration (Barry et al., 2013; Danabalan et al., 2022). The transportation of natural gas that feeds seeps can be broken down into a slow and steady continuous diffusive flux (dissolved in water) (Marschall et al., 2005; Cheng et al., 2021; Cheng et al., 2023), a rapid potentially episodic phase buoyancy-driven flow dependent on tectonic history (Brown, 2000; Rice, 2022) or a combination of both. Episodic seepage describes systems that are sporadic and advective in nature such as instances of venting or enhanced tectonic activity versus those that are continuous such as a steady diffusive flux (Araktingi et al., 1984; Abrams, 1992; Arp, 1992a, 1992b; Jones and Burtell, 1996; Klusman and Saeed, 1996; Brown, 2000; Brown, 2000; Abrams, 2020a; Rice, 2022). Various authors have advocated against the importance of diffusion as a significant transport method for natural gases citing insufficient fluxes and extremely long charging periods (i.e., hundreds of millions of years) (Davis, 1967; Smith et al., 1971; Hunt, 1979; Rice, 2022). It is important to note that migration will follow the zones of least resistance based on pressure drive, buoyancy drive and capillary resistance; and observed seeps do not have to occur directly over subsurface gas accumulations (Abrams, 2020b).

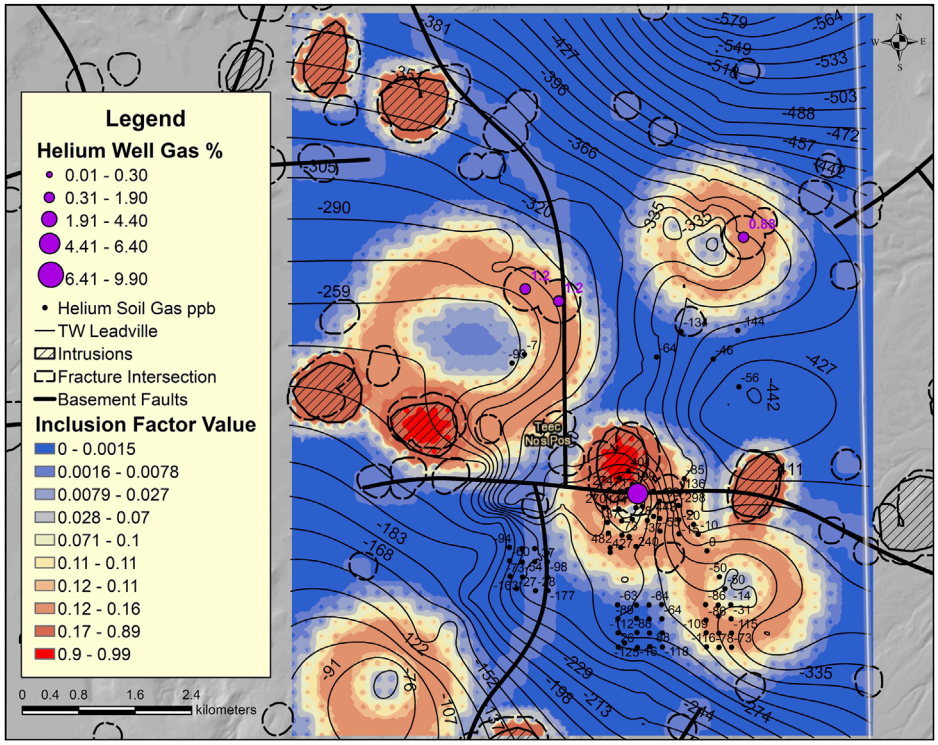

FIGURE 10
Predictive model derived from Bayesian ANOVA inclusion factors shows He-potential in extended areas mapped around Tohache Wash on the Mississippian Leadville Limestone (C.I. 15 m). The model highlights two hot zones colored bright red (the highest predicted likelihood of encountering subsurface He-rich gas).

Based on the soil gas mapping, the Tohache Wash area is likely a combination of both types of fluxes (advective and diffusive). Regarding indications for advective buoyancy-driven fluxes, there is evidence for differential compaction controlled faulting/fluid flow in the geospatial distribution of He soil gas signatures around the flanks of the structure (Figure 5). In this scenario, the reservoir pressure exceeds the capillary pressures in the seal and He escapes the reservoir. This means the gas would be forced through limited pathways in a seal (effusion zones) and be subjected to subsequent advection in the overlying sediments. Indications for diffusion are the spherical dispersion patterns observed on the surface at Tohache Wash (Figure 5) and the Tom and Akah Nez areas as well (Supplementary Figures S3, S4) (Price, 1986). Thus, the Tohache Wash area, which shows higher He signatures on the flanks of structures and semi-spherical surface He signatures in Figure 5, a high reservoir He % (Supplementary Table S3), and the strongest He soil gas survey signatures, can be a prime example of an advection-diffusion based system where the reservoir pressure is greater than the capillary pressure. Given it has the highest He soil gas values measured, coupled with the fact that it has had consistent He % well tests over decades (1969 and 2016) despite having been produced (~13% of original gas), shows that there must still be a significant reservoir of He at depth and that it is not subjected to an extremely rapid loss mechanism, otherwise the accumulation would not exist with such high He values (Supplementary Table S4).

Examining the He soil gas mapping, the Porcupine Dome area, Beautiful Mountain and Rattlesnake fields are likely the result of advection-driven fluxes with minimal contributions from diffusion. A characteristic of diffusion dominated processes is that generally diffusion has nearly spherical dispersion pattern that can't be focused into localized anomalies (Price, 1986), which is not what is observed from the soil gas surveys (i.e., more linear trends demarcating basement fault zones) for parts of the Porcupine Dome area, Beautiful Mountain Field and Rattlesnake Field. The strong linear pattern of soil signatures at the Porcupine Dome area and the depleted nature of the Beautiful Mountain and Rattlesnake fields suggests there is a rapid process (likely advective buoyancy-driven flow) controlling gas migration from reservoir to surface (Figures 6–8). Although diffusion is likely occurring, there is not strong evidence that diffusion alone for the depleted fields is a significant mechanism.

Specifically, for the Beautiful Mountain and Rattlesnake fields, the soil gas surveys indicate large gaps or depletion zones (i.e., lack of He signal greater than air) where there should be higher He anomalies if there was a substantial amount of He remaining in the reservoir (Figures 6, 7). Plausible reasons explaining the lack of surface signatures for depleted fields (either through gas cap depletion, production/movement of groundwater, inadequate reservoir pressure or some other factor) are presented in Section 5.4.

Using original helium in place (OHIP) and external and internal flux calculations (Robinson and Peng, 1976; Mireault et al., 2007; Buttitta et al., 2020), the average age of all the accumulations is calculated to be ~30 Ma, which corresponds to documented Oligocene volcanism in the region (Gonzales and

Lake, 2017; Halford et al., 2022) (Supplementary Table S4). This volcanism/tectonic activity likely served as the catalyst in the creation of these gas accumulations, (i.e., pressure differences driving He exsolution from a dissolved state in groundwater). Therefore, given the regional tectonic history of the Colorado Plateau which has provided prevalent fracture and fault pathways, it seems unreasonable to assume diffusion loss would be a dominant process to explain vertical migration for any systems in the area, and other mechanisms such as buoyancy-driven advective mass transport should be considered as the dominant transport mechanism (Brown, 2000; Huitt, 1956; Happel and Brenner, 1965; Brodkey, 1967; Horwitz, 1969; MacElvain, 1969; Allen, 1984; Churchill, 1988; Rice, 2022) (Supplementary Information S5).

5.3.1 Near surface migration microseepage model

Upon analyzing the structural and geochemical data, a schematic (Figure 9) is presented, which highlights the main elements impacting vertical microseepage of He migration from a gas reservoir to the surface. Patterns observed on the surface (quantified with soil gas He surveys) can be used to distinguish characteristic geometries related to apical anomalies (immediately above a subsurface gas body) and halo anomalies (spill points around a subsurface gas body) (Abrams, 2020b). Apical and halo anomalies can provide useful information about the trapping potential and subsurface architecture of the reservoir. Additionally, geologic migration pathways (basement faults, thrust faults, diapirs, fractured basin carrier beds, etc.) can act as advection-driven pathways allowing higher concentrations of He seepage on the surface. Regarding the most notable interpretations, there is evidence for pathway-driven migration in the Beautiful Mountain Field (Figure 6), Rattlesnake Field (Figure 7), and Porcupine Dome area (Figure 8); partial vertical halos are observed in the Tohache Wash area (Figure 5) and Beautiful Mountain Field (Figure 6); and vertical apical anomalies are observed in the Tohache Wash area (Figure 5).

5.4 Applications for helium exploration

Below several scenarios are presented to be used as a guide (not all inclusive) when interpreting He concentration measurements from soil gas data for He exploration. While the labeling of He values is subjective and will vary for different geographic regions, for the purpose of this study and to explore different plausible mechanisms for gas migration, high He signals are those >300 ppb above the background air level, moderate He signals are those between 100–300 ppb, and low He signals are those between 40–100 ppb.

It is important to note that the presence of a He signature in the soil does not definitely indicate an economic accumulation of He in the subsurface as have been documented in the literature in active volcanic areas (Barberi and Carapezza, 1994; D'Alessandro and Parello, 1997; Padron et al., 2012; Padron et al., 2013). Simply observing He is not enough to identify a resource and in fact may indicate a failed resource, or it may not be conclusive. However, utilizing soil gas geochemistry within the context of knowing the geology (e.g., trapping structures and seals at depth) combined with other factors such as the spatial relationship of structures can be helpful to identify the reason for the He migration. In certain contexts the soil gas signals can be useful, but may also provide overlapping signatures that need to be differentiated. Therefore, soil gas geochemistry is only a tool, and should be used with other techniques to help reduce risk in exploration for underground resources.

5.4.1 High He surface signals

Regarding exploration frameworks, the presence of strong halo signatures with high He concentrations (advective transport controlled) could indicate an economically viable He accumulation at depth. The higher the soil He signal is, the more likely a robust He accumulation could be present in the subsurface. This approach coupled with data from historical He reservoir tests can provide information regarding He accumulations at depth. Although all reservoirs in this study are leaking to some degree for there to be a recordable He soil surface signature (Rice, 2022), it is likely these leakage rates are too minor/slow to deplete most fields if there are no active/open fault zones cross-cutting the reservoir and if there was an adequate initial amount of gas in the reservoir. This supposition can be strengthened with repeated high He tests (e.g., Tohache Wash) over a prolonged period of time (several decades). Thus, this scenario of high He signals observed at the surface could indicate a He-rich subsurface reservoir and therefore be ideal for He prospecting.

5.4.2 Moderate-low He surface signals

The moderate-low He concentrations measured at the surface could be indicative of a reservoir that has lost significant amounts of gas due to initial production and subsequent gas has been lost (i.e., gas leakage due to faults) meaning it is no longer economically viable. We consider a scenario of rapid He loss (e.g., Rattlesnake and Beautiful Mountain fields) involving the depletion of a natural gas cap and initial liquids. In this scenario, the initial gas cap was extensively produced, and remaining initial liquids that could have been acting as a buffer slowing down He loss were additionally lost. A proposed mechanism for this buffering is liquid blocking or impeding pore throats, which effectively lowers permeability at the gas cap – reservoir seal boundary (Lin et al., 2022; Rice, 2022). However, once the liquid barrier was removed, pore throat pathways were left open, which resulted in an increase in permeability (i.e., increased migration through fractures/faults). This process could explain why despite such high initial He % tests, there are no He-rich zones where the pilot wells were drilled and produced as the He flux (e.g., vertical migration) leaving the reservoir exceeded that which was entering it.

Another scenario to explain a moderate-low He concentration surface signal involves the production and/or movement of groundwater to permeable zones (e.g., Rattlesnake Field and Porcupine Dome, respectively). Excess reservoir water production indicates that that a water cone or water fingering can develop due to pressure differentials (Arthur, 1944). More specifically, the water that is drawn upwards from underlying/adjacent wet rock to the wellbore, can push the remaining unproduced reservoir gas to the fractured edges of the structural uplift (e.g., Rattlesnake Field). Additionally, regarding groundwater movement, gas can be transported via advection of subsurface fluids along open fault zones (e.g., Porcupine Dome's thrust fault). Once gas encounters

these zones of higher permeability, the capillary pressure in the seal will be lower than the underlying reservoir, and the gas and adjacent fluid can migrate upwards via advection/buoyancy out of the reservoir (Rice, 2022). This scenario, which could result in He gas depletion depending on the influence of the groundwater pressure drive, is plausible as there are observed He soil gas signatures at the edge of the Rattlesnake structure where there are likely (micro)fractures due to high stress (point of maximum curvature) and where there is a mapped thrust fault in the Porcupine Dome area.

Thus, these scenarios of observed moderate-low surface signals could indicate a leaky seal and be unideal for He prospecting. Caution should be given to such systems to mitigate risk.

5.4.3 Low-no He signals

An additional explanation for the lack of a strong or moderate surface He signal is due to the lack of adequate reservoir pressure. Because in theory if a well was produced for a short amount of time (e.g., parts of the Rattlesnake Field, Porcupine Dome, and Beautiful Mountain Field), the reservoir pressure would fall below the capillary pressure and no significant amounts of He would be escaping the reservoir. This means the gas would not be forced through limited pathways in a seal (effusion zones) and not be subjected to subsequent diffusion or advection in the overlying sediments. This scenario could in theory describe reservoirs that have good potential, but would require further mass balance models to estimate reservoir potential for He.

5.4.4 No He signals

Another plausible explanation for the lack of He surface signals, is that there were simply never any substantial amounts of He in the subsurface reservoirs to begin with or it was not concentrated to reach economic levels. This scenario of no He signals above background air values could indicate zones that have relatively nonexistent He potential and thus be unideal for He exploration efforts.

5.5 Case study of Tohache Wash: predictive framework model

In addition to the Tohache Wash area being considered a prime target for exploration by having the highest He surface signatures, the area is chosen for further statistical modeling because of the availability of geological data, high He % well tests (1969 and 2016), and likely slow He leakage in some areas (i.e., greater He preservation). The primary objective of building a predictive framework model is to identify key He-system criteria, understand the relative importance of the He-system variables, and subsequently search for He-potential in extended areas mapped around Tohache Wash in the Mississippian Leadville Limestone reservoir. More specifically, the goal is to observe if a Bayesian ANOVA statistical analysis, given suitable training data, could effectively aid in the interpretation of soil gas data in the context of He exploration. Building on He probability predictive modeling (Halford et al., 2024), a similar approach to determine He-gas rich areas is utilized by constructing a predictive framework, but with the addition of He soil gas data, high density fracture networks, and localized structural mapping of reservoirs (from 2D seismic and well control).

Ultimately, the Bayesian ANOVA model examines the effects of independent variables (i.e., structural features and historical data) on the dependent variable (i.e., He soil gas values) and observes the effects of multiple predictors. Based on Bayesian ANOVA statistical models, the most critical migration element of the He-system in the Tohache Wash area are intrusive bodies (Table 1). These bodies can behave similar to basement faults as they act as migration conduits that support advective buoyancy-driven transport from basement granitic source rocks into overlying sediments (Danabalan et al., 2022; Halford et al., 2022; Halford et al., 2024). Regarding the most critical trapping variable, reservoir flank, the presence of He surface anomalies on reservoir flanks suggest that there are likely faults and associated fractures as a result of differential compaction of the reservoir (Table 1). This has implications in understanding the role that subsurface structural architecture has on trapping/accumulation potential of the reservoir and deciphering potential He prospectivity of an area.

By examining real world geological data, often the elements of a He-system are not standalone (Craddock et al., 2017; Brennan et al., 2021; Halford et al., 2022; Danabalan et al., 2022), rather they build on each other similar to those in a petroleum system (Selley and Sonnenberg, 2015). Namely, the presence of an intrusion as a migration conduit/pathway, and a reservoir flank structure to aid in trapping is often not enough to produce a He anomaly. Thus, in order to construct an updated predictive model from the Bayesian ANOVA statistical models using Tohache Wash area variables and data, the computed BF inclusion coefficients (Table 1) are utilized for all variables from the initial Bayesian ANOVA model to act as the weighting factors (quantitatively rank each variable) for the updated predictive model (Figure 10).

Upon examining the predictive model (Figure 10), there are two areas with the highest likelihood of encountered He based on the BF inclusion coefficients. The highest predicted region corresponds directly with the area of the Navajo Z-1 well (API: 02001053090001), which has produced 6% He. This indicates that the model is well calibrated with real world data producing a He hot zone where it would be expected. The model indicates a new area of high-He potential that is ~2.5 km immediately west of the Navajo Z-1 well. Concerning the flexibility of the model, the exact buffer zones around each variable can be adjusted and updated (e.g., when more data are acquired), which allows the model to be highly versatile and adaptable. Thus, given suitable training data, Bayesian ANOVA statistical analysis, can help interpret soil gas data in the context of He exploration. Additionally, the model represents a significant development from the initial observations of Andreason et al. (2022), by producing quantitative interpretations of sampled field areas and by utilizing model predictions to extrapolate patterns in field areas which were not sampled.

This model is significant in that it essentially generates target areas for new/further He exploration and development. Another important aspect of this approach is that it allows a site by site specific model that can be constructed with real world data in order to extrapolate subsurface He gas plays. This approach is beneficial where there is well and seismic data to produce

reservoir structure maps plus geochemical and geophysical data to integrate/tie data from the surface to the basement and to assess the viability of a He-system. The utility of this predictive model in areas outside of the Four Corners Plateau is great especially in areas that have experienced some level of geologic and tectonic activity. An important note is that the model is not the only solution/approach to represent data and create quantitative statistical predictions, but we hope it will be used as a starting point to allow further development of He exploration modeling.

6 Conclusion

The importance of structural features influencing advective based migration pathways for subsurface He accumulations has been established (Halford et al., 2024), but these observations were drawn from a widely scattered database of historical He % in subsurface reservoir gas. Until now, the He data to determine exactly how vital these features and their relevant processes are in controlling a He accumulation was not available. Fortunately, there are new data from soil gas surveys to examine geospatial relationships and test the efficacy of surficial soil surveys in He exploration. By combining historical geochemical data, well log data, 2-D seismic data and potential field geophysical data, structural features and their relationships to closely spaced measured He soil concentrations were identified and subsequently tested.

As geospatial relationships are being examined within the soil gas survey data, it is important to understand the mechanisms that allow the He in the subsurface reservoir to migrate into the soil. In several fields interpreted basement faults act as migration conduits from the basement to the surface (i.e., leaky reservoirs) producing He microseepages, and in other cases there is evidence that He surface signatures are controlled by reservoir flank/crest fracturing likely due to differential compaction. Based on the regional geologic history, advection-driven systems are likely responsible for the observed He soil gas signatures.

To examine the relative importance of geologic elements and their relevant processes, the most prospective area (i.e., Tohache Wash) is modeled. Prospectivity at Tohache Wash is based on the area's highest soil gas measurements, multiple high He well tests, high He retention potential, and the availability of geological data. Bayesian ANOVA models predict the most significant variables controlling He occurrences are intrusions and flanks of the reservoir, which provide additional information related to the migration and trapping of He. Using Bayesian inclusion coefficients, a predictive model is computed using weighted variables, which is constructed with historical data that inputs predicted variables and translates them into a visualization of areas where there are likelihoods of high and low He. This model produces an output that matches historical records of an anomalous zone and also highlights an additional area of interest for future exploration.

Thus, in order to more effectively explore for subsurface He accumulations at a finer scale, surficial soil gas surveys can be used to provide a closer examination of helium's response to structural features in hopes of finding and developing future He plays when combined with other techniques such as well data, seismic data, geochemical data, and potential field geophysical data. The significance of this approach is that it ties geological data throughout various depths of the crust (basement, reservoir, and surface) to examine He-systems. Translating this predictive model into other areas where there is sufficient well and seismic data to map reservoirs can be a powerful tool to mitigate exploration risk.

Data availability statement

Publicly available datasets were analyzed in this study. Helium geochemical data supporting this research is included in Brennan et al. (2021) - doi: 10.5066/P92QL79J, Halford (2018) (https://repository.mines.edu/handle/11124/172822), Halford (2023) - doi: 10.5287/ora-00zdnvm4m, and Halford et al. (2022) - doi:10.1016/j.chemgeo.2022.120790. Maps of the high-resolution geophysical data and related geochemical data supporting this research can be found in Andreason et al. (2022) (https://nnogc.com/wp-content/uploads/2024/04/FINAL-REPORT-HELIUM-NAVAJO-NATION_APR2022.pdf). Additional inquiries should be directed to the corresponding author and the Navajo Nation Division of Natural Resources, Navajo Minerals Department, and the Navajo Nation and Navajo Nation Oil and Gas Co.

Author contributions

DH: Conceptualization, Formal Analysis, Methodology, Visualization, Writing–original draft, Writing–review and editing. RK: Conceptualization, Formal Analysis, Methodology, Supervision, Writing–review and editing. JD: Formal Analysis, Project Administration, Resources, Writing–review and editing. BC: Formal Analysis, Methodology, Visualization, Writing–review and editing. MC: Formal Analysis, Methodology, Visualization, Writing–review and editing. Dalton DB: Methodology, Writing–review and editing. MA: Formal Analysis, Methodology, Writing–review and editing. GR: Formal Analysis, Methodology, Writing–review and editing.

Funding

The author(s) declare financial support was received for the research, authorship, and/or publication of this article. Research was supported by the University of Oxford Noble Laboratory, the University College Oxford-Radcliffe Scholarship, and the Division of Energy and Mineral Development (Bureau of Indian Affairs).

Acknowledgments

We are thankful for the Navajo Nation and Navajo Minerals Department for their support. We are grateful for the independent release of preliminary Navajo Nation data and evaluation into the public domain in April of 2024 provided by NNOGC from an internal study (unrefereed preprint) funded with an Energy and Mineral Development Program (EMDP) grant from Division

of Energy and Mineral Development under the U.S. Bureau of Indian Affairs. The preprint served as the foundation for our new scientific paper, providing the raw data, preliminary figures, notes, and methodology information. We thank NNOGC and Navajo tribal members for collecting the soil gas samples, and for contracting the data to be analyzed (GeoFrontiers Corp.). We kindly thank the comments and inputs from Walter D'Alessandro and Gilles Levresse. Discussions and comments from Mike Kendall, Chris Ballentine, Roberto Betancourt-Castro, Ralph Nelms, MariaLuz Duran, and Cassidy Wolfe benefited this work.

Conflict of interest

Author RK was employed by Snowfox Discovery. Authors BC and MC were employed by Earthfield Technology LLC. Authors DB and GR were employed by GeoFrontiers Corporation. Author MA was employed by Navajo Nation Oil and Gas Company.

The remaining authors declare that the research was conducted in the absence of any commercial or financial relationships that could be construed as a potential conflict of interest.

Publisher's note

All claims expressed in this article are solely those of the authors and do not necessarily represent those of their affiliated organizations, or those of the publisher, the editors and the reviewers. Any product that may be evaluated in this article, or claim that may be made by its manufacturer, is not guaranteed or endorsed by the publisher.

Supplementary material

The Supplementary Material for this article can be found online at: https://www.frontiersin.org/articles/10.3389/feart.2024.1434785/full#supplementary-material

References

Abrams, M. A. (1992). Geophysical and geochemical evidence for subsurface hydrocarbon leakage in the Bering Sea, Alaska. *Mar. Petroleum Geol. Bull.* 9 (2), 208–221. doi:10.1016/0264-8172(92)90092-s

Abrams, M. A. (2020a). Marine seepage variability and its impact on evaluating the surface migrated hydrocarbon seep signal. *Mar. Petroleum Geol.* 121, 104600. doi:10.1016/j.marpetgeo.2020.104600

Abrams, M. A. (2020b). *Microseepage vs. Macroseeepage: defining seepage type and migration mechanisms for differing levels of seepage and surface expressions*. USA: AAPG Datapages, Inc.

Allen, J. R. L. (1984). *Sedimentary structures their character and physical basis*. New York, NY: Elsevier 1, 593.

Allis, R. G., Chidsey, T. C., Morgan, C., Moore, J., and White, S. (2003). "CO2 sequestration potential beneath large power plants in the Colorado Plateau-Southern Rocky Mountain region, USA," in Second Annual Conference on Carbon Sequestration, NETL Proceedings, China, May 5-8, 2003.

Andreason, M. W., Cathey, B., Cathey, M., and Rice, G. K. (2022). Identification and maturation of new potential helium deposits on the Navajo nation lands, internal grant deliverable by the Navajo Nation Oil and Gas Co., Earthfield Technology LLC and GeoFrontiers Corp. funded by an EMDP grant #A21AP10056 awarded to the Navajo Nation. [Preprint]. Available at: https://nnogc.com/wp-content/uploads/2024/04/FINAL-REPORT-HELIUM-NAVAJO-NATION_APR2022.pdf.

Araktingi, R., Benefield, M., Bessenyei, Z., Coats, K., and Tek, M. (1984). Leroy storage facility, Uinta County, Wyoming: a case history of attempted gas-migration control. *Journal of Petroleum Technology* 34, 132–140. doi:10.2118/11180-PA

Arp, G. W. (1992a). Effusive microseepage: a first approximation model for light hydrocarbon movement in the subsurface. *Assoc. Petroleum Geochem. Explor. Bull.* 8, 1–17.

Arp, G. W. (1992b). An integrated interpretation for the origin of the Patrick Draw oil field sage anomaly. *AAPG Bull.* 76, 301–306. doi:10.1306/bdff87d6-1718-11d7-8645000102c1865d

Arthur, M. G. (1944). Fingering and coning of water and gas in homogeneous oil sand. *Trans. AIME* 155 (01), 184–201. doi:10.2118/944184-g

Baars, D. L. (1983). Rattlesnake mississippian (gas), T. 29 N., R. 19 W., NMPM, san juan county, New Mexico. *Four Corners Geol. Soc. Oil Gas Fields Four Corners Area* III, 1006–1007.

Ball, N. L., and Snowdon, L. R. (1973). *A preliminary evaluation of the applicability of the helium survey technique to prospecting for petroleum*. Canada: Geological Survey of Canada, 199–202. Paper 73-1B.

Ballentine, C. J., Burgess, R., and Marty, B. (2002). Tracing fluid origin, transport and interaction in the crust. *Rev. Mineralogy Geochem.* 47, 539–614. doi:10.2138/rmg.2002.47.13

Barberi, F., and Carapezza, M. L. (1994). Helium and CO2 soil gas emission from Santorini (Greece). *Bull. Volcanol.* 56, 335–342. doi:10.1007/BF00326460

Barry, P. H., Hilton, D. R., Fischer, T. P., de Moor, J. M., Mangasini, F., and Ramirez, C. (2013). Helium and carbon isotope systematics of cold "mazuku" CO_2 vents and hydrothermal gases and fluids from rungwe volcanic province, southern Tanzania. *Chem. Geol.* 339, 141–156. doi:10.1016/j.chemgeo.2012.07.003

Bayarri, M. J., Berger, J. O., Forte, A., and García-Donato, G. (2012). Criteria for Bayesian model choice with application to variable selection. *Ann. Statistics* 40 (3), 1550–1577. doi:10.1214/12-AOS1013

Bjorlykke, K., and Hoeg, K. (1997). Effects of burial diagenesis on stresses, compaction, and fluid flow in sedimentary basins. *Mar. Petroleum Geol.* 14 (3), 267–276. doi:10.1016/S0264-8172(96)00051-7

Blackwelder, E. (1920). The origin of the central Kansas oil domes. *AAPG Bull.* 4, 89–94. doi:10.1306/3d932536-16b1-11d7-8645000102c1865d

Boreham, C. J., Edwards, D. S., Poreda, R. J., Darrah, T. H., Zhu, R., Grosjean, E., et al. (2018). Helium in the Australian liquefied natural gas economy. *J. Aust. Petroleum Prod. Explor. Assoc. (APPEA)* 58 (1), 209–237. doi:10.1071/AJ17049

Brennan, S., East, J., Dennen, K., Jahediesfanjani, H., and Varela, B. (2021). Helium concentrations in United States wells. *U.S. Geol. Surv. Sci. Investig. Rep.* 5, 2021–5085. doi:10.5066/P92QL79J

Brister, B. S., and Allen, L. G. (2002). *New Mexico's Energy, Present and Future—Policy, Production, Economics, and the Environment*. San Juan Basin: New Mexico Bureau of Geology and Mineral Resources Decision-Makers Field Guide, 152.

Broadhead, R. F., and Gillard, L. (2004). Helium in New Mexico: geologic distribution and exploration possibilities. *N. M. Bureau Geol. Mineral Resour. A Div. N. M. Tech, Socorro, N. M.* Open File Report No. 483. doi:10.58799/OFR-483

Brodkey, R. S. (1967). *The phenomena of fluid motions*. Reading, MA: Addison-Wesley Publishing, 737.

Brown, A. (2000). Evaluation of possible gas microseepage mechanisms. *AAPG Bull.* 84 (11), 1775–1789. doi:10.1306/8626C389-173B-11D7-8645000102C1865D

Brown, H. H. (1978). Beautiful Mountain mississippian (oil), T. 26-27 N., R. 19 W., NMPM san juan county, New Mexico. *Four Corners Geol. Soc. Oil Gas Fields Four Corners Area* I-II, 207–208.

Buczkowski, D. L., and Cooke, M. L. (2004). Formation of double-ring circular grabens due to volumetric compaction over buried impact craters: implications for thickness and nature of cover material in Utopia Planitia, Mars. *J. Geophys. Res. Planets* 109. doi:10.1029/2003JE002144

Buttitta, D., Caracausi, A., Chiaraluce, L., Favara, R., Gasparo Morticelli, M., and Sulli, A. (2020). Continental degassing of helium in an active tectonic setting (northern Italy): the role of seismicity. *Sci. Rep.* 10, 162. doi:10.1038/s41598-019-55678-7

Cheng, A., Sherwood Lollar, B., Gluyas, J. G., and Ballentine, C. J. (2023). Primary N_2-He gas field formation in intracratonic sedimentary basins. *Nature* 615 (7950), 94–99. doi:10.1038/s41586-022-05659-0

Cheng, A., Sherwood Lollar, B., Warr, O., Ferguson, G., Idiz, E., Mundle, S. O. C., et al. (2021). Determining the role of diffusion and basement flux in controlling ^{4}He distribution in sedimentary basin fluids. *Earth Planet. Sci. Lett.* 574, 117175. doi:10.1016/j.epsl.2021.117175

Chidsey, T. C., Jr. (2020). The Mississippian Leadville Limestone oil and gas play, Paradox Basin, southeastern Utah and southwestern Colorado—lisbon field, regional, and analog studies. *Utah Geol. Surv. Bull.* 139, 246. doi:10.34191/B-139

Churchill, S. W. (2002). *Viscous flows: the practical use of theory*. Boston: Butterworths Publishers, 602.

Clyde, M. A. (2018). BAS: bayesian adaptive sampling for bayesian model averaging. (Version 1.5.3)[Computer software].

Corcoran, P. L. (2008). Ordovician paleotopography as evidenced from original dips and differential compaction of dolostone and shale unconformably overlying Precambrian basement on Manitoulin Island, Canada. *Sediment. Geol.* 207 (1-4), 22–33. doi:10.1016/j.sedgeo.2008.04.003

Craddock, W. H., Blondes, M. S., DeVera, C. A., and Hunt, A. G. (2017). Mantle and crustal gases of the Colorado Plateau: geochemistry, sources, and migration pathways. *Geochimica Cosmochimica Acta* 213, 346–374. doi:10.1016/j.gca.2017.05.017

D'Alessandro, W., and Parello, F. (1997). Soil gas prospection of He, 222Rn and CO2: vulcano Porto area, Aeolian islands, Italy. *Appl. Geochem.* 12 (2), 213–224. doi:10.1016/S0883-2927(96)00066-2

Danabalan, D., Gluyas, J. G., Macpherson, C. G., Abraham-James, T. H., Bluett, J. J., Barry, P. H., et al. (2022). The principles of helium exploration. *Pet. Geosci.* 28 (2), 2021–2029. doi:10.1144/petgeo2021-029

Davis, G. H., and Bump, A. P. (2009). "Structural geologic evolution of the Colorado Plateau," in *Backbone of the americas: shallow subduction, plateau uplift, and ridge and terrane collision*. Editors S. M. Kay, V. A. Ramos, and W. R. Dickinson (America: Geological Society of America Memoir), 204, 99–124. doi:10.1130/2009.1204(05

Davis, J. B. (1967). *Petroleum microbiology*, 604. Germany: Elsevier. doi:10.1017/S001675680004930X

Dawson, M. K. (1983). Akah Nez devonian (oil), T. 23 N., R. 20 W., NMPM, san juan county. *N. M. Four Corners Geol. Soc. Oil Gas Fields Four Corners Area* III, 918–919.

Debnam, A. H. (1969). Geochemical prospecting for petroleum and natural gas in Canada. *Geol. Surv. Can. Bull.* 177, 1–26.

Dyck, W. (1976). The use of helium in mineral exploration. *J. Geochem. Explor.* 5 (1-2), 3–20. doi:10.1016/0375-6742(76)90031-5

Friedman, I., and Denton, E. H. (1976). A portable helium sniffer. *J. Res. U.S. Geol. Surv.* 4 (1), 35–36. doi:10.3133/ofr75532

Gay, A., Lopez, M., Cochonat, P., Levache, D., Sermondadaz, G., and Seranne, M. (2006a). Evidences of early to late fluid migration from an upper Miocene turbiditic channel revealed by 3D seismic coupled to geochemical sampling within seafloor pockmarks, Lower Congo Basin. *Mar. Petroleum Geol.* 23, 387–399. doi:10.1016/j.marpetgeo.2006.02.004

Gay, A., Lopez, M., Cochonat, P., Seranne, M., Levache, D., and Sermondadaz, G. (2006b). Isolated seafloor pockmarks linked to BSRs, fluid chimneys, polygonal faults and stacked Oligocene–Miocene turbiditic palaeochannels in the Lower Congo Basin. *Mar. Geol.* 226 (1), 25–40. doi:10.1016/j.margeo.2005.09.018

Gonzales, D. A., and Lake, E. T. (2017). Geochemical constraints on mantle-melt sources for Oligocene to Pleistocene mafic rocks in the Four Corners region, USA. *Geosphere* 13 (1), 201–226. doi:10.1130/GES01314.1

Halford, D. T. (2018). *Isotopic analyses of helium from wells located in the Four Corners area, southwestern, USA*. Master's Thesis (USA: Colorado School of Mines). Available at: https://repository.mines.edu/handle/11124/172822>.

Halford, D. T. (2023). Geologic processes that control sourcing and migration of subsurface helium. *Univ. Oxf.* PhD thesis. doi:10.5287/ora-00zdnvm4m

Halford, D. T., Karolytė, R., Andreason, M. W., Cathey, B., Cathey, M., Dellenbach, J. T., et al. (2024). Probabilistic determination of the role of faults and intrusions in helium-rich gas fields formation. *Geochem. Geophys. Geosystems* 25 (60), e2024GC011522. doi:10.1029/2024GC011522

Halford, D. T., Karolytė, R., Barry, P. H., Whyte, C. J., Darrah, T. H., Cuzella, J. J., et al. (2022). High helium reservoirs in the Four Corners area of the Colorado plateau, USA. *Chem. Geol.* 596, 120790. doi:10.1016/j.chemgeo.2022.120790

Happel, J., and Brenner, H. (1965). *Low Reynolds number hydrodynamics with special applications to particulate media*, 553. Englewood Cliffs, New Jersey: Prentice-Hall.

Holland, P. W. (1984). *An analyzer for determining helium-4 in the parts-per-billion range, report of investigations 8853*. USA: U.S. Bureau of Mines, 14.

Horwitz, L. (1969). "Hydrocarbon geochemical prospecting after 20 years," in *Unconventional methods in exploration for petroleum and natural gas*. Editor W. Heroy (Dallas: Southern Methodist University Press), 205–218.

Huitt, J. L. (1956). Fluid flow in simulated fractures. *American Institute of Chemical Engineers Journal* 2 (2), 259–264.

Hunt, J. M. (1979). *Petroleum geochemistry and geology*, 615. San Francisco: W. H. Freeman and Company.

Ireland, M. T., Goulty, N. R., and Davies, R. J. (2011). Influence of stratigraphic setting and simple shear on layer-bound compaction faults offshore Mauritania. *J. Struct. Geol.* 33 (4), 487–499. doi:10.1016/j.jsg.2010.11.005

JASP Team (2023). JASP [Computer software]. Available at: https://jasp-stats.org/.

Jones, V. T., and Burtell, S. G. (1996). "Hydrocarbon flux variations in natural and anthropogenic seeps," in *Hydrocarbon migration and its near-surface expression*. Editors D. Schumacher, and M. Abrams (USA: AAPG Memoir), 66, 203–221. doi:10.1306/M66606C16

Karolytė, R., Warr, O., Van Heerden, E., Flude, S., De Lange, F., Webb, S., et al. (2022). The role of porosity in H_2/He production ratios in fracture fluids from the Witwatersrand Basin, South Africa. *Chem. Geol.* 595, 120788. doi:10.1016/j.chemgeo.2022.120788

Klusman, R., and Saeed, M. (1996). "Comparison of light hydrocarbon mechanisms," in *Hydrocarbon migration and its near-surface expression*. Editors D. Schumacher, and M. Abrams (London: AAPG Memoir), 66, 157–168.

Koide, H., and Bhattacharji, S. (1975). Formation of fractures around magmatic intrusions and their role in ore localization. *Econ. Geol.* 70, 781–799. doi:10.2113/gsecongeo.70.4.781

Liang, F., Paulo, R., Molina, G., Clyde, M. A., and Berger, J. O. (2008). Mixtures of g priors for bayesian variable selection. *J. Am. Stat. Assoc.* 103, 410–423. doi:10.1198/016214507000001337

Lin, T., Tan, C., Zhang, X., Zhao, L., Wei, H., Wang, L., et al. (2022). Characteristics of pore-throat in tight sandstones of the jurassic ahe formation in the northern tarim basin. *Geofluids* 2022, 1–18. Article ID 1139232, 18. doi:10.1155/2022/1139232

Lorenz, J. C., and Cooper, S. P. (2003). Tectonic setting and characteristics of natural fratures in Mesaverde and Dakota reservoirs of the San Juan Basin. *N. M. Geol.* 25 (1), 3–14. doi:10.58799/NMG-v25n1.3

Lundstern, J. E., and Zoback, M. D. (2020). Multiscale variations of the crustal stress field throughout North America. *Nat. Commun.* 11, 1951. doi:10.1038/s41467-020-15841-5

MacElvain, R. (1969). "Mechanics of gaseous ascension through a sedimentary column," in *Unconventional methods in exploration for petroleum and natural gas*. Editors W. Heroy (Dallas: Southern Methodist University Press), 15–28.

Mackintosh, S. J., and Ballentine, C. J. (2012). Using ^{3}He/^{4}He isotope ratios to identify the source of deep reservoir contributions to shallow fluids and soil gas. *Chem. Geol.* 304–305, 142–150. doi:10.1016/j.chemgeo.2012.02.006

Malinowski, M. J. (1983). Tom devonian (oil), T. 25 N., R. 19 W., NMPM, san juan county, New Mexico. *Four Corners Geol. Soc. Oil Gas Fields Four Corners Area* III, 1050–1053.

Marschall, P., Horseman, S., and Gimmi, T. (2005). Characterisation of gas transport properties of the opalinus clay, a potential host Rock Formation for radioactive waste disposal. *Oil Gas Sci. Technol.* 60 (1), 121–139. doi:10.2516/ogst:2005008

Mehl, M. G. (1920). The influence of the differential compression of sediments on the attitude of bedded rocks. *Sci. New Ser.* 51, 520.

Meng, Q., and Hodgetts, D. (2020). Forced folding and fracturing induced by differential compaction during post-depositional inflation of sandbodies: insights from numerical modelling. *Mar. Petroleum Geol.* 112, 104052. doi:10.1016/j.marpetgeo.2019.104052

Merriam, D. F. (1999). "Plains-type folds" in the Mid-continent region (U.S.A.): chronicling a concept. *Earth Sci. Hist.* 18 (2), 264–294. doi:10.17704/eshi.18.2.p510p244704346j8

Mireault, R., Dean, L., Esho, N., Kupchenko, C., Mattar, L., Morad, K., et al. (2007). Reservoir engineering for geologists. canadian society of petroleum geologists reservoir magazine. Available at: http://large.stanford.edu/courses/2013/ph240/zaydullin2/docs/fekete.pdf.

Moore, R. C. (1920). The relation of burial granite in Kansas to oil production. *AAPG Bull.* 4, 255–261. doi:10.1306/3D932544-16B1-11D7-8645000102C1865D

Mtili, K. M., Byrne, D. J., Tyne, R. L., Kazimoto, E. O., Kimani, C. N., Kasanzu, C. H., et al. (2021). The origin of high helium concentrations in the gas fields of southwestern Tanzania. *Chem. Geol.* 585, 120542. doi:10.1016/j.chemgeo.2021.120542

Nyberg, B., Nixon, C. W., and Sanderson, D. J. (2018). NetworkGT: A GIS tool for geometric and topological analysis of two-dimensional fracture networks. *Geosphere* 14 (4), 1618–1634. doi:10.1130/GES01595.1

Padron, E., Perez, N. M., Hernandez, P. A., Sumino, H., Melian, G., Barrancos, J., et al. (2012). Helium emission at Cumbre Vieja volcano, La Palma, Canary Islands. *Chem. Geol.* 312-313, 138–147. doi:10.1016/j.chemgeo.2012.04.018

Padron, E., Perez, N. M., Hernandez, P. A., Sumino, H., Melián, G. V., Barrancos, J., et al. (2013). Diffusive helium emissions as a precursory sign of volcanic unrest. *Geology* 41 (5), 539–542. doi:10.1130/G34027.1

Price, L. (1986). "A critical overview and proposed working model of surface geochemical exploration," in *Unconventional methods in exploration for petroleum and natural gas IV*. Editor M. J. Davidson (United States: Southern Methodist University Press), 245–304.

Re, G. (2017). *Evolution and dynamics of a monogenetic volcanic complex in the southern Hopi buttes volcanic field (AZ, US): magma diversion and fragmentation processes at the jagged rocks complex (thesis, doctor of philosophy)*. USA: University of Otago. Available at: http://hdl.handle.net/10523/7358.

Reimer, G. M. (1976). Design and Assembly of a Portable Helium Detector for Evaluation as a Uranium Exploration Instrument. *USGS Open-File Rep.* 76-398, 18. doi:10.3133/ofr76398

Rice, G. (2022). Vertical migration in theory and in practice. *Interpretation* 10 (1), SB17–SB26. doi:10.1190/INT-2020-0216.1

Roberts, A. A., and Roen, J. B. (1985). *Near surface helium anomalies associated with faults and gas accumulations in western Pennsylvania, United States Department of the Interior*. Kolkata: Geological Survey. Open File Report 85-546.

Robinson, D. B., and Peng, D. Y. (1976). A new two-constant equation of state industrial and engineering chemistry: fundamentals. *Industrial Eng. Chem. Fundam.* 15, 59–64. doi:10.1021/i160057a011

Rouder, J. N., Engelhardt, C. R., McCabe, S., and Morey, R. D. (2016). Model comparison in ANOVA. *Psychonomic Bull. and Rev.* 23, 1779–1786. doi:10.3758/s13423-016-1026-5

Rusciadelli, G., and Di Simone, S. (2007). Differential compaction as a control on depositional architectures across the Maiella carbonate platform margin (central Apennines, Italy). *Sediment. Geol.* 196 (1), 133–155. doi:10.1016/j.sedgeo.2006.06.006

Selley, R. C., and Sonnenberg, S. A. (2015). *Elements of petroleum geology*. 3rd Edition. Amsterdam: Elsevier, 507.

Smith, J. E., Erdman, J. G., and Morris, D. A. (1971). "Migration, accumulation and retention of petroleum in the earth," in *Proceedings of the 8th world petroleum congress*. Moscow: Applied Science Publishers, 13–26.

Spencer, C. W. (1978). Tohache Wash Area (Helium), T. 41 N., R. 30 E., GandSRM, Apache County, Arizona. Four corners geological society. *Oil Gas Fields Four Corners Area* I-II, 92–93.

Taouki, I., Lallier, M., and Soto, D. (2022). The role of metacognition in monitoring performance and regulating learning in early readers. *Metacognition Learn.* 17 (3), 921–948. doi:10.1007/s11409-022-09292-0

van den Bergh, D., van Doorn, J., Marsman, M., Draws, T., van Kesteren, E.-J., Derks, K., et al. (2020). A tutorial on conducting and interpreting a Bayesian ANOVA in JASP. *L'Année Psychol.* 120 (1), 73–96. doi:10.3917/anpsy1.201.0073

van Doorn, J., van den Bergh, D., Böhm, U., Dablander, F., Derks, K., Draws, T., et al. (2021). The JASP guidelines for conducting and reporting a Bayesian analysis. *Psychonomic Bull. Rev.* 28, 813–826. doi:10.3758/s13423-020-01798-5

Wagenmakers, E. J., Love, J., Marsman, M., Jamil, T., Ly, A., Verhagen, J., et al. (2018). Bayesian inference for psychology. Part II: Example applications with JASP. *Psychonomic Bull. and Rev.* 25 (1), 58–76. doi:10.3758/s13423-017-1323-7

Werner, R. T. (1953). Interpretation of magnetic anomalies at sheet-like bodies. *Sveriges Geologiska Undersok, Series C, Arsbok* 43 (6), 413–449.

Williams, S. R. J. (1987). Faulting in abyssal-plain sediments, Great Meteor East, Madeira Abyssal Plain. *Geol. Soc. Lond. Spec. Publ.* 31 (1), 87–104. doi:10.1144/GSL.SP.1987.031.01.08

Woodward, L. A. (1973). "Structural framework and tectonic evolution of the Four Corners region of the Colorado Plateau," in *Monument Valley*. Editor H. L. James (Guidebook: New Mexico Geological Society), 94–98. doi:10.56577/FFC-24.94

Woodward, L. A., Anderson, O. J., and Lucas, S. G. (1997). "Tectonics of the Four Corners region of the Colorado Plateau," in *Mesozoic geology and paleontology of the Four Corners region*. Editors O. J. Anderson, B. S. Kues, and S. G. Lucas (Mexico: New Mexico Geological Society, Guidebook, 48th Field Conference), 57–64. doi:10.56577/FFC-48.57

Xu, S., Hao, F., Xo, C., Wang, Y., Zou, H., and Gong, C. (2015). Differential compaction faults and their implications for fluid expulsion in the northern Bozhong Subbasin, Bohai Bay Basin, China. *Mar. Petroleum Geol.* 63, 1–16. doi:10.1016/j.marpetgeo.2015.02.013